AN ABSTRACT OF THE THESIS OF

Nataliia Pylypiuk for the degree of Master of Science in Chemistry presented on September 7, 2011

Title: Improvements in Synthesis and Response Techniques of Ion-Selective Sensors.

Abstract approved:

_____

Vincent T. Remcho

Two improvements to the established procedures for synthesis and response detection of ion-selective optical sensors (optodes) were introduced.

The first improvement addresses the drawback of organic dye (optode-localized chromoionophore) photobleaching. This positively impacts fluorescence response and allows for (1) direct measurement of hydrogen ion activity upon binding with the dye, or (2) indirect measurement of sodium activity (when complexed by a second ionophore, highly selective to sodium ions) that competes with protons for ion-exchange sites inside the optode.

To accomplish this, quantum dots (QDs), semiconductor nanocrystals characterized by a high resistivity to photobleaching, were incorporated in the polymer matrix together with all necessary sensing components to serve as "soft" light-source donors (via the inner filter effect) to excite chromoionophores (acceptors). It was shown that this method is appropriate for fluorescent signal (response) measurement while maintaining stability, calibration with respect to pH, and calibration with respect to sodium activity.

The second improvement focused on optimization of the synthesis of optodes. Ion-selective sensors have a relatively short life-time due to photobleaching of the organic dye component of the system. Since the common solvent displacement method

employed in the one-step, batch procedure for optode synthesis is not appropriate for "on-demand" synthesis, a microfluidic approach for quasi-continuous synthesis was introduced. An additional benefit of this approach is greater facility for control of particle size distribution.

The microfluidic "chip" was fabricated on a cyclic olefin copolymer (COC) substrate by micromilling the channels to meet the fluid distribution requirements of the process, then sealing the chip by clamping in a home-made fixture. It was discovered that the size of the particle may be determined by the polymer concentration in one of the reacting solutions, while flow rate changes and component ratios were determined not to directly affect the particle size. The microfluidic platform proved to be a convenient tool for optode fabrication.

For the calibration and cell penetration experiments with the optodes, the microfluidic platform was coupled with a second microfluidic "chip" that facilitated optode trapping with the help of laser tweezers.

Improvements in Synthesis and Response Techniques of Ion-Selective Sensors

by

Nataliia Pylypiuk

A THESIS

Submitted to

Oregon State University

In partial fulfillment of

the requirements for the

degree of

Master of Science

Presented September 7, 2011

Commencement June 2012

Master of Science thesis of Nataliia Pylypiuk

Presented on September 7, 2011

APPROVED:

_____

Major Professor, representing Chemistry

_____

Chair of the Department of Chemistry

_____

Dean of the Graduate School

I understand that my thesis will become part of the permanent collection of Oregon State University libraries. My signature below authorizes release of my thesis to any reader upon request.

_____

Nataliia Pylypiuk, Author

ACKNOWLEDGEMENTS

I am greatly thankful to my research advisor, Dr. Vincent Remcho, for his endless support throughout my graduate studies. It was honor for me to work under his supervision. Without his guidance this thesis would not be possible. Thank you for making me a part of ambitious Remcho's research group.

I would like to acknowledge the Ukrainian division of Fulbright Graduate Program for awarding me with outstanding scholarship and providing the funding support for my first two years of study.

I appreciate the time and commitment of my graduate committee members: Kim Anderson, Paul Blakemore and Christopher Beaudry.

Enormous thank you goes to Valeriya Bychkova for her emotional support. She was with me in all the ups and downs of the research, always ready to give a valuable advice.

I say a special gratitude to Myra Koesdjojo: first, for warm welcoming to the group and then for teaching me everything she knows about microfluidics, for her bright ideas and supervision.

I am thankful to Todd Miller and Jack Rundel from Oregon Nanoscience and Microtechnologies Institute (ONAMI) for all the help with microfluidic platform construction.

Thank you to all my group members: Dao Nammoonnoy, Esha Chatterjee, Yolanda Tennico, Tae-Hyeong Kim, Adeniyi Adenuga, Yuanyuan Wu. It was such a pleasure to work with all of you.

I would like to acknowledge the Department of Chemistry, staff and faculty for providing a friendly environment upon my studies and research work.

This is also a great opportunity to express special respect to my first MS advisor – Volodymyr Zaitsev from Taras Shevchenko National University of Kyiv. Under his direct supervision I learned all the research skills needed in analytical chemistry and was encouraged to continue my education overseas.

Finally, I wish to say thank you to my aunt Lena for her endless support and unconditional love.

CONTRIBUTION OF AUTHORS

Dr. Vincent Remcho provided assistance in interpreting data, editing and writing this dissertation. Valeriya Bychkova was my co-laborator and assisted with all the data collection. Myra Koesdjojo worked with me on microfluidics projects and is a co-author of all the ideas.

TABLE OF CONTENTS

Page

1. Introduction.....1
1.1 Ion-selective optical sensors.....2
1.1.1 Application of ion-selective optical sensors.....2
1.1.2 Structure of ion-selective optical sensors.....3
1.2 Introduction to quantum dots.....5
1.2.1. Properties of quantum dots.....5
1.2.2. Application of quantum dots.....7
1.3 Introduction to microfluidics.....8
1.3.1 Introduction.....8
1.3.2 Design of microfluidics platforms.....9
1.3.3 Fabrication of microfluidics platforms.....9
1.3.4 Channel formation techniques.....12
1.3.5 Bonding of microfluidic platform.....13
1.4 References.....14

2. Improvement in response of ion-selective optical sensors.....18
2.1 Introduction.....19
2.2 Experimental.....23
2.2.1 Reagents.....23
2.2.2 Membrane composition.....24
2.2.3 Membrane cocktail preparation.....25
2.2.4 Polymer film preparation.....25
2.2.5 Synthesis of ion-selective optical sensors.....26
2.2.6 Optics.....26

TABLE OF CONTENTS (Continued)

Page

2.2.7 Spectral recording 27
2.2.8 Zeta-potential measurements 27
2.2.9 Calibration.....27
2.2.10 Calculations.....27
2.2.11 Calibration curves 27
2.2.12 Limits of detection 28
2.3 Results.....28
2.4 Conclusion 39
2.5 References.....39

3. Improvement in synthesis of ion-selective optical sensors.....40
3.1 Introduction.....41
3.2 Experimental.....43
3.2.1 Microfluidic platform fabrication 43
3.2.2 Chemicals for optodes synthesis.....44
3.2.3 Size distribution measurements 45
3.3 Results and discussion 45
3.3.1 Design of microfluidic platform 45
3.3.2 Choice of substrates.....46
3.3.3 Fabrication of the microfluidic platform.....46
3.3.4 Bonding method for the microfluidic platform.....47
3.3.5 Microfluidic platform-to-world connections 48
3.3.6 Reagent delivery 49
3.3.7 Batch-mode synthesis of optodes.....49

TABLE OF CONTENTS (Continued)

Page

3.3.8 Synthesis of optodes using the microfluidic platform 50

3.3.9 Fabrication of microfluidic platform for laser tweezers trapping 54

3.4 Conclusions.....57

3.5 References.....57

4. Summary and conclusions 58

LIST OF FIGURES

Figure Page

1.1 Typical structure and response mechanism of ion-selective optodes 3

1.2 Example of absorption and emission spectra of QDs 5

1.3 General structure of QDs 6

1.4 Size-tunable emission of QDs.....7

2.1 Fluorescence spectra of protonated and deprotonated forms of chromoionophore I.....20

2.2 Approximate absorption and emission spectra of chromoionophore I.....21

2.3 Diagram illustrating optode response via the inner filter effect 22

2.4 Explanation of ISO/QD response based on inner filter effect 22

2.5 TEM images of Qdots.....24

2.6 Absorbance spectra of protonated and deprotonated forms of chromoionophore I (ETH5294) 29

2.7 Spectra of QD_{545} and QD_{605} generated by Invitrogen's SpectraViewer software.....29

2.8 White precipitation upon membrane cocktail addition to QDs in decane 30

2.9 Invitrogen ITK organic QDots 545, 605, 655 in decane (original solvent) and THF (replaced solvent) 31

2.10 Invitrogen's ITK organic Qdots at different pH 31

2.11 pH-dependence of QDs fluorescence in optodes membrane prepared as polymer film 32

LIST OF FIGURES (Continued)

Figure Page

2.12 Fluorescence spectra of optodes that contain chromoionophore I and QD_{655} upon excitation at 350 nm and 535 nm; pH=7 33

2.13 Fluorescence spectra of optode membrane as a polymer film at pH=6.0 and pH=9.0.....34

2.14 The solvent displacement method leads to the production of uniform optode microspheres 35

2.15 Pictorial representation of optode synthesis by the solvent displacement method 35

2.16 pH-dependence of QDs fluorescence optodes' membrane prepared as a polymer film and spherical particles 36

2.17 Calibration of polymer films with the respect to pH. 37

2.18 Calibration of polymer films with the respect to Na^+ activity 38

3.1 Particles size dependence on the type of polymer used for the synthesis 41

3.2 Effect of polymer concentration in THF on the size of the particles 42

3.3 Design of proposed microfluidic platform. 45

3.4 Micromilled (on COC) plates of microfluidic platform. 47

3.5 Laser-cut 60 μm nozzle 47

3.6 PC+PET fixture used for microfluidic platform assembly 48

3.7 Effect of polymer concentration on particle size distribution for optodes synthesized via batch method in acetone 50

3.8 Fluorescence images of the optodes synthesized using microfluidic platform 51

LIST OF FIGURES (Continued)

Figure Page

3.9 Effect of polymer concentration on the size distribution of optodes synthesized in a microfluidic reactor 51

3.10 Comparison of the effects of the polymer concentration in acetone on the sized distribution of the optodes synthesized by batch and microfluidic methods 52

3.11 Particle size dependence on a flow rate ratio.....53

3.12 Effect of the flow rate ration on the sized distribution of the optodes synthesized by batch and microfluidic method.....54

3.13 Explanation of particle trapping by laser tweezers.....54

3.14 Microfluidic platform design for on-line trapping of the optodes after the synthesis process.....55

3.15 Microfluidic platform for trapping.....56

3.16 Explanation of the final device for intracellular ion activity measurements.....56

LIST OF TABLES

Table Page

1.1. Comparison of main characteristics of polymers typically used for microfluidic purposes.....11

2.1. Structural formulas of the components of sodium-selective optode.....25

CHAPTER 1

INTRODUCTION

1.1. Ion-selective optical sensors.

1.1.1. Application of ion-selective optical sensors.

Ion-selective optical sensors (ISO sensors, or simply *optodes*) are members of an extensive family of nano/microsensors commonly referred to as PEBBLEs (Photonic Explorers for Biomedical use with Biologically Localized Embedding). PEBBLEs is a general term that encompasses a variety of fabrication techniques for miniaturization of well-known sensors [1].

Optodes leverage the same response mechanisms as ion-selective electrodes, contain identical components and became popular as intracellular sensors in early 1990s following key developments pioneered by the Kopelman research group [2].

Optodes have found broad use in medicine and biology due to their most obvious feature - small size. To introduce any kind of sensor into a cell with the goal of making a measurement un-influenced by the measurement tool, one should seek to minimize (ideally eliminate) perturbation. Even when the tip diameter of the probe is small (only hundreds of nanometers) the penetration volume of the tip is sufficient to occupy a significant part of the cell volume. A simple solution to this problem is to use not probes, but spherical sensors of micrometer to nanometer diameter. In this case the perturbation volume is almost negligible and, at the same time, sensors retain high surface-to-volume ratio for an easy access of target molecules.

Medical application of optodes is of interest due to the known fact that ideal concentrations of ions such as Na^+, K^+, and H^+ in living organisms are strictly defined and any changes in their values may be indicative of disease. Ion-selective sensors offer the advantage of directly measuring *activities* of free ions in the biological matrix, in contrast to the widely popular fluorescence methods that represent total ion *concentrations*. Another benefit of ISO's is that it is feasible to design them for sensitivity to any ion for which a complexing ionophore is available. The work described in this thesis was devoted to cation-selective sensors.

The generally accepted sensing mechanism of cation-selective ISO's is based on a competition between two ions (primary/target ion and reference ion) for a limited number

of ion-exchange sites (given that the concentration of ion-exchanger is limited) inside the optode matrix.

1.1.2. Structure of ion-selective optical sensors.

Typically, cation-selective optodes consist of a plasticized polymer matrix, an ionophore that is highly selective to the target ion (cation), an ion exchanger (R) to facilitate mass transport of ions through the cell membrane, and an organic dye (chromoionophore) having optical properties that change upon protonation/deprotonation (Figure 1.1).

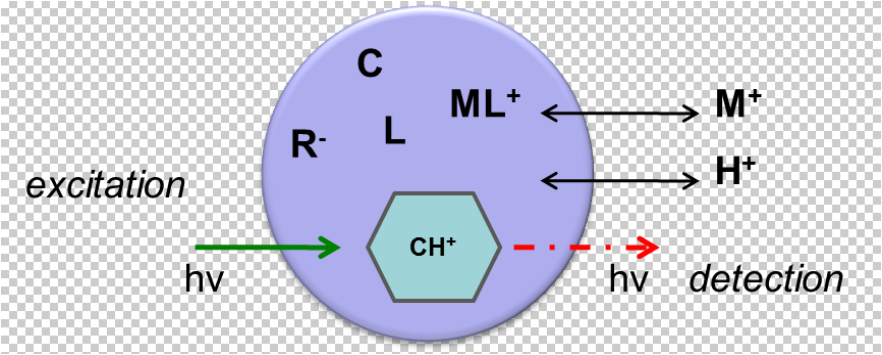

Figure 1.1. Typical structure and response mechanism of ion-selective optodes.

The three sensing components of the sensors can be incorporated into an inert polymer matrix that protects the cellular environment from direct interaction with the chemicals and guards the sensing components from potential protein-binding, etc. The size of the sensors is sufficient, relative to the size of the organic dyes (10-15 nm), to give rise to the possibility of incorporating multiple labels (organic dyes) to provide ratiometric measurements [3].

Poly(vinyl chloride) (PVC) is the most widely used polymer matrix for optode production due to its low cost and good mechanical properties. However, the glass transition temperature (T_g) of PVC is 80-85^0 C; thus, to achieve a fluid membrane PVC must be plasticized. Normally, polymer membranes are composed of one part (by weight) PVC and two parts of plasticizer [4]. This high plasticizer content allows the plasticizer to serve also as a solvent for all the sensing components of the ISO; thus, the plasticizer must be chemically compatible with all of them [5]. Dioctyl sebacate (DOS) is a

plasticizer prevalently used for PVC. Also advantageous is that the PVC performs as semi-permeable membrane; hence, the target ion can easily diffuse through it.

The primary ISO sensing component is the selective ionophore. The ionophore contains oxygen and nitrogen atoms that serve as electron donors and has an inner cavity that ideally matches the size of the target ion. Calixarenes – cyclic oligomers of phenol-formaldehyde condensates – have been used as ionophores for many years owing to the ease with which they are synthesized and their particularly good complexing properties [6]. The work presented here is focused largely on sodium-selective ISO's, therefore as a main sensing component sodium ionophore was used. Thus an anionic additive (tetraphenylborate salt) served as the obligate ion-exchanger. Sodium ISO's are among the most widely used in clinical studies since Na^+-channels are involved in many important cellular functions [7].

Since most ionophores are optically inactive, in order to get an optical signal from an ISO, an additional optically-active component (chromoionophore [8]) must be introduced to the system. Chromoionophore is typically a lipophilized pH-indicator, thus it does not complex cations other than H^+ and is compatible with the lipophilic media inside the optode. The chromoionophore undergoes distinct changes in absorption or fluorescence induced by ion-exchange equilibrium shifts inside the membrane.

Sensor response is determined by the competition between two ions (in our system, the cation of interest and a second cation, usually H+) for ion-exchange sites in the polymer matrix. This means that if the pH of the sample is constant (a buffered solution), the optode indirectly responds to the metal activity in the sample and vice versa. When the target analyte is extracted into the membrane, the optical (fluorescent) properties of the optodes are changed due to protonation or deprotonation of the fluorescent dye. This in turn serves as an effective tool for the signal detection. Hence, the optodes *directly* detect any change in the pH of the sample and *indirectly* detect changes in primary ion activity.

1.2. Introduction to quantum dots.

1.2.1. Properties of quantum dots

Quantum dots (QDs) are semiconductor nanocrystals 2-10 nm in diameter that consist of elements from the periodic groups II-VI, III-V, IV-VI. They have spherical or bullet-like form and a set of unique optical properties that make QDs very promising tools for bioimaging [9] and fluorescent labeling. In comparison with organic dyes, QDs have narrow, tunable (to a specific wavelength of interest, based on the size of the QD) ideally symmetric emission spectra [10] that allow easy separation of fluorescent signal from the excitation light [11]. QDs also have broad absorption spectra (Figure 1.2) that make it possible to excite nanocrystals of different sizes (and thus with different emission peaks) using a single excitation source [12]. Moreover, QDs are more resistant to optical signal degradation with time during excitation (e.g., photobleaching) than well-known organic dyes [13]. The latter benefit allows applications where longer imaging time is involved.

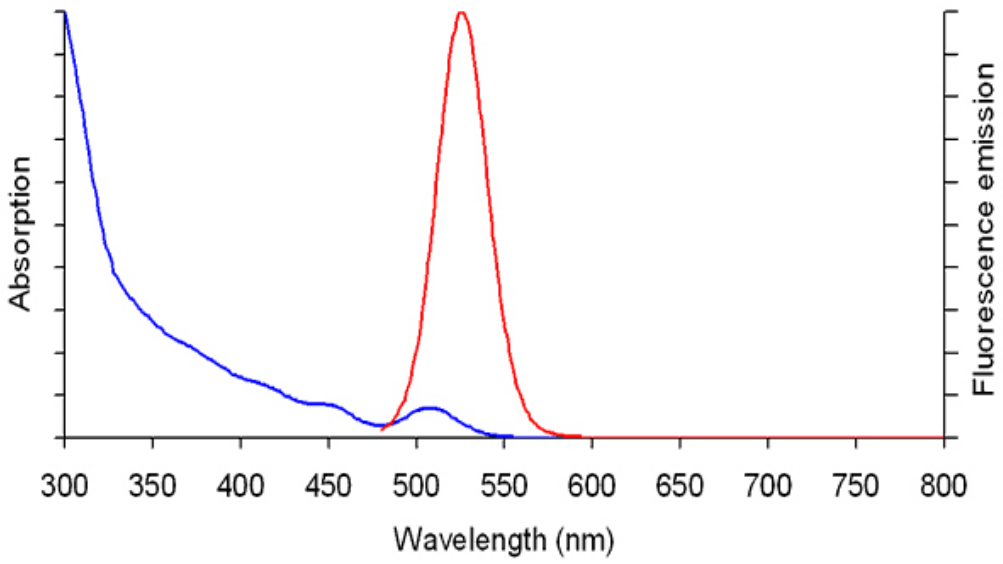

Figure 1.2. Example of absorption (blue) and emission (red) spectra of QDs.

Typically, QDs are composed of (Figure 1.3):

- a solid core (usually cadmium chalcogenide; CdSe is the most widely used due to the availability of reactants and the simplicity of crystallization) that determines QD color;
- a passivation shell (inorganic wide-band semi-conductor, usually ZnS due to its widest band-gap) that prevents non-radiative deactivation [14] and thus improves brightness and stability [15];
- a hydrophobic organic coating (usually tri-*n*-octylphosphine or its oxide – TOP/TOPO) to reduce cytotoxicity and provide the possibility of functionalization if needed.

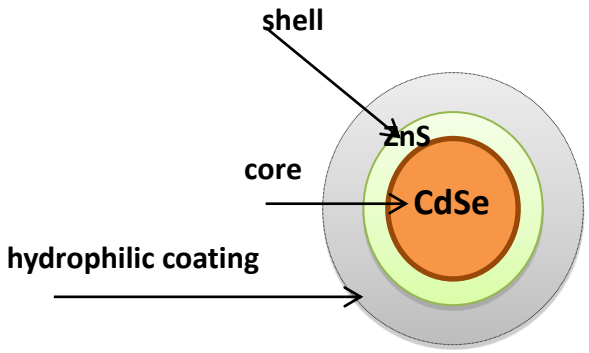

Figure 1.3. General structure of QDs.

Fluorescence of QDs is caused by the recombination of photogenerated electron-hole pairs [16], and begins with absorption of a photon with excitation energy higher than the bandgap of the QD. This excites an electron from the valence band to the conduction band and thus causes hole formation. The electron then relaxes back from its excited state to the normal state with emission of light (fluorescence). While the absorbed energy can be of any value greater than the bandgap, the emitted energy is proportional to the bandgap (this proportionality explains why the emission spectrum is so narrow, with full width at half-maximum around 20-40 nm) and decreases with an increase in nanocrystal size, leading to a longer emission wavelength. The latter explains the unique absorption-emission properties of QDs.

1.2.2. Application of quantum dots

As was briefly mentioned above, QDs have found their best application in imaging of biological specimens owing to their superior stability and resistance to phtobleaching relative to organic dyes.

The possibility of fine tuning QD emission characteristics (Figure 1.4) made possible the use of nanocrystals as donors in photochemically-induced fluorescence [17].

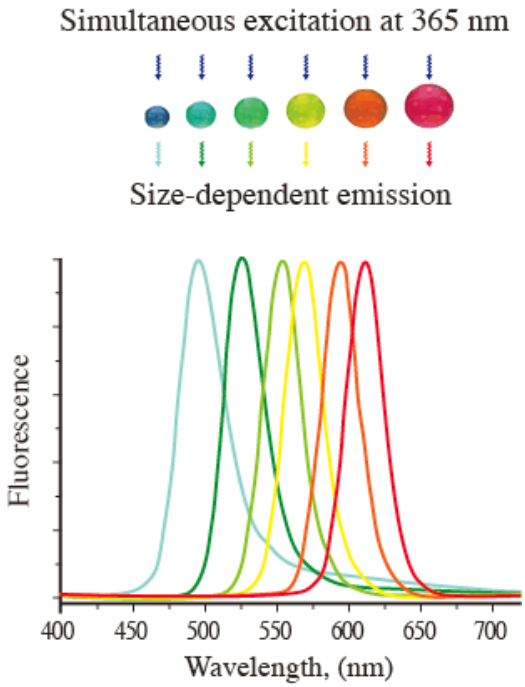

Figure 1.4. Size-tunable emission of QDs [18].

This, coupled with the broad absorption spectra typical of QDs, made possible an approach to *indirectly* excite organic dyes (acceptor) in situations where *direct* excitation is forbidden or not preferable [19]. Two known phenomena are utilized for this purpose.

Fluorescence (or Förster) Resonance Energy Transfer (FRET) is a non-radiative excitation transfer between two parts of molecule that are separated from each other by a distance that is greater than the sum of their van der Waals radii [20]. By adding organic coatings to QDs, it is possible to tailor nanocrystals to meet specific FRET purposes [21]. This has led to the creation of a wide variety of sensors. For instance, Wang et al. reported on a silica based analytical nanosphere ratiometric sensor (ANSor) [22] for local

pH-monitoring. Later, water-soluble QDs were used as donors in sodium sensors to measure sodium activities in 0-130 nM solutions [23].

An alternative approach to FRET is to utilize the inner filter effect (IFE). This phenomenon is based on the decrease of emission intensity due to the reabsorption of emitted energy by another molecule. The IFE differs from FRET in that the two species involved in the energy exchange are not attached to each other, but simply co-exist in the sample. Tohda et al. utilized IFE to detect non-fluorescent (but absorbing) molecules using fluorescent organic dyes as energy donors [24]. Dubach et al. demonstrated the possibility to incorporate QDs into the polymer matrix of ion-selective sensors together with a fluorescent dye, and utilized IFE for signal detection [25]. In this case the organic dye (fluorophore) was excited by light emitted from QDs, thus QD fluorescence signal intensity was quenched and served to provide an indirect measurement of ion activity in the solution. Ruedas-Rama et al. reported CdSe/ZnS photoluminescence lifetime-based nanosensors [26] with a linear pH response in the range of 5.2-6.9 that can be used in intracellular media. A similar sensor was built for monitoring of sodium response from 0.0001 to 0.1 M at pH 4.8 [27].

1.3. Introduction to microfluidics

1.3.1. Introduction

The term “microfluidic” was introduced to describe the behavior of fluids (and methods to control this behavior) at the micrometer scale [28]. This trend has become very popular in analytical chemistry over the past ten years. In analytical and synthetic studies, miniaturization provide for several distinct advantages:

- reduced time of synthesis/analysis;
- reduced consumption of reagents;
- reaction conditions (flow rates, concentrations) can be readily changed;
- easy sample handling;
- portability [29].

Basically, all the sample manipulations (detection/separation/analysis) can be done on one small (cm range) microfluidic platform (or simply “chip”) [30].

1.3.2. Design of microfluidic platforms

Construction of a microfluidic platform begins with an appropriate design. Any kind of engineering (AutoCad, SolidWorks, etc.) or graphical (Microsoft Paint) software may be used to draw a pattern with defined channel dimensions and then applied toward manufacturing according to a chosen fabrication method.

When designing microfluidic mixers or platforms for synthesis, one should take into account the Reynolds number (a parameter that characterizes the type of flow in the channel, and is directly proportional to the size of the channel and the average flow rate). The Reynolds number for a liquid flowing in a microfluidic channel at low velocity is low ($R<100$), which means that the flow inside the channel is not turbulent (turbulence begins to occur at $R>2000$) but laminar, thus mixing in the channel is dictated only by diffusion. Since the sizes of channels in microfluidic platforms are small, one of the ways to create turbulence and enhance mixing is to operate at high flow rates while seeking to avoid high backpressure.

1.3.3. Fabrication of microfluidic platforms

Thermoplastic polymers (polymers that can be molded at their glass transition temperature {T_g}, and retain the molded shape after cooling below T_g [31]) have become the most common substrates for microfluidic device fabrication in this decade. While glass and silicon, which were heavily used in the preceding decade, offer good chemical compatibility, they are expensive and demand comparatively complicated processing techniques. Hence, the transition to readily available, relatively cheap polymers was economically preferable and enabled mass-production of cost-effective and disposable microfluidic platforms.

Among the vast variety of polymers a few materials have gained higher attention:

1. *Polydimethylsiloxane* (PDMS) [32] is optically transparent, has low auto-fluorescence and can be prepared with a desired hardness that is based on the amount of added curing agent. This is the only elastomer that is widely used among more convenient thermoplastics. The drawback of PDMS is its hydrophobic surface and swelling in the presence of organic solvents.

Additionally, PDMS platforms have limited pressure and temperature operating ranges (low mechanical strength) and are gas permeable.

2. *Poly(methyl methacrylate)* (PMMA) is robust, mechanically stable and optically transparent. Its surface can be easily modified to suit desired analytical needs. At the same time it has low resistivity to organic solvents.
3. *Polycarbonate* (PC) is usually used as substitution for PMMA, but is more glass-like and is less robust (delaminates at high pressure).
4. *Polyethylene terephthalate* (PET) is the only polymer with excellent chemical resistivity to both acids/bases and organic solvents. It can be opaque (which is not good for microfluidic platforms due to prevalence of optical detection in such systems) or transparent (usually sold in thin sheets). Even though the latter type seems ideal for microfluidic fabrication, this PET is very rigid and can be difficult to process.
5. *Cyclic olefin copolymer* (COC) is glass-like transparent polymer with high transmission in the UV, low autofluorescence, good mechanical properties, low water uptake and, what is very important for the synthesis process, has excellent chemical compatibility [33]. COC is resistant to hydrolysis, acids, polar solvents (alcohols, ketones). T_g of COC can vary from 75^0 C to 175^0 C depending on the nonborene content.

The properties of these key polymers are summarized in the table below for comparison (Table 1.1.).

Table 1.1. Comparison of main characteristics of polymers typically used for microfluidic purposes [34].

Polymer		T_g, ^{0}C	Color	Resistance		Trade name
abbreviation	name			organic solvents	acids/bases	
PMMA	poly(methyl methacrylate)	100-122	transparent	good	good	Plexiglass
PC	polycarbonate	145-150	transparent	good	good	Makrolon
PET [35]	polyethylene terephthalate	70-80	transparent/opaque	excellent	excellent	Mylar
PS	polystyrene	100-105	transparent	poor	good	Polystyrol
COC [36]	cyclic olefin copolymer	75-170	transparent	excellent	good	Topas, Zeonex

1.3.4. Channel formation techniques.

Among a remarkable variety of channel formation techniques there are a few methods that provide particularly satisfactory results when applied to polymers.

Soft photolithography with subsequent hot embossing [37]. This method consists of the following steps:

1) primary master fabrication (layer of photoresist is spin-coated on a substrate (silicon, glass), shaped with photomask and cross-linked);

2) secondary master fabrication (features from the cured photoresist are transferred to the polymer with high T_g by hot-embossing, e.g. heating the polymer substrate to the temperature just above T_g and applying a small pressure);

3) final microfluidic platform fabrication (features from the secondary master are transferred to the polymer with lower T_g by hot-embossing).

This technique is time consuming and limited mostly to academic use [38].

Laser cutting. In this technique, energy from a laser is focused to break polymer bonds and thus cut the channel. This makes it possible to avoid the time-consuming steps of master preparation and hot-embossing. The disadvantage of this method is that it is hard to tune the laser intensity for a needed penetration depth. Moreover, the laser leaves burn marks on the sides of a channel. The imperfections affect flow and sorptive interactions adversely.

Printer/cutter use. Another cutting method, but in this case channels are cut on thin substrates (paper, PC sheets) using a high-precision commercial X-Y knife cutter, as is often employed in the sign- and decal-manufacturing industry.

Micromilling/micromachining. Recently, highly precise and small diameter (down to 50μm) machine tools have become available, making possible the direct cutting of desired features on a substrate. Microfluidic designs can be drawn in any available and suitable software package and program-cut into a polymer substrate [39]. The main

advantage of this method is that channels can be cut on practically any known material or type of polymer.

1.3.5. Bonding of microfluidic platforms

Typically, microfluidic features are cut on one or both parts of polymer substrate that must later be bonded together to form ready-to-use, closed channel platforms. The following techniques have found widespread use in bonding adjacent layers of fluidic devices.

Thermal bonding. Polymer plates are heated to a temperature very close to their T_g. When the material begins to flow, polymeric chains from the two substrates diffuse into one other and thus bond (a small pressure may be applied to ensure a quality bond). This is the simplest way to bond two polymer pieces together, but it does require careful application of heat at temperatures close to T_g, which increases the probability of collapsing the pre-made microfluidic features [40].

Surface modification. In this method surface of polymer is treated with oxygen-plasma [41], sometimes with additional post-treatment with chemicals (silane reagents [42]), prior to applying a small pressure. O_2-plasma treatment is utilized in order to improve the adhesive properties of the surface. This method works well on microfluidic platforms with relatively small bonding areas.

Solvent welding. One polymer piece is covered with a thin film of solvent that attacks the surface and softens it enough to bond to another polymer piece when they are pressed together. In this case, as previously discussed with the thermal bonding, the most crucial step is to prevent microfluidic channel deformation [43].

"Fixturing". While the methods mentioned above are the types of direct bonding (polymer substrates are bonded together more or less permanently), fixturing and the following methods are examples of indirect, less-permanent bonding. A "fixture" is a

platform (usually hand-made) that consists of two plates made of metal or plastic with fasteners on the perimeter to clamp the two parts of a microfluidic “chip” together.

Double-sided tape. A polymer plate is covered with a thin layer (<100 μm) of double-sided adhesive tape avoiding the pre-cut microfluidic features (sometimes these features can be cut into the tape along with the polymer substrate) and then two pieces of the microfluidic platform are pressed together.

Channel formation and bonding technique choice depends not only on the type of polymer substrate that is to be used for microfluidic fabrication, but also on tools and reactants available in the laboratory, the projected end-use of the channel, and the solvents or gases to which the system will be exposed when in use.

1.4. References.

[1] Buck, S., H. Xu, M. Brasuel, M. Philbert, and R. Kopelman. "Nanoscale probes encapsulated by biologically localized embedding (PEBBLEs) for ion sensing and imaging in live cells." *Talanta* 63 (2004): 41-59.

[2] Sasaki, K., Zy Shi, R. Kopelman, and H. Masuhara. "Three-dimensional PH Microprobing with an Optically-manipulated Fluorescent Particle." *Chem. Lett.* 25: 141-145.

[3] Lee, Y.-E., R. Smith, and R. Kopelman. "Nanoparticle PEBBLE Sensors in Live Cells and in Vivo." *Annu.. Rev. Anal. Chem.* 2 (2009): 57-76

[4] Moody, G., R. Oke, and J. Thomas. "A calcium-sensitive electrode based on a liquid ion exchanger in a poly(vinyl chloride) matrix." *Analyst* 95 (1970): 910-918.

[5] Johnson, D., and Leonidas Bachas. "Ionophore-based ion-selective potentiometric and optical sensors." *Anal. Bioanal. Chem.* 376 (2003): 328-341.

[6] Cadogan, A.Dermot Diamond, Malcolm R. Smyth, Mary Deasy, M. Anthony McKervey, and Stephen J. Harris. "Sodium-selective Polymeric Membrane Electrodes Based on Calix[4]arene Ionophores." *The Analyst* 114.12 (1989): 1551.

[7] Woodhull, An. "Ionic Blockage of Sodium Channels in Nerve." *J.Cell Biology* 61.6 (1973): 687-708 .

[8] Seiler, K., and W. Simon. "Theoretical Aspects of Bulk Optode Membranes." *Anal. Chim. Acta* 266 (1992): 73-87.

[9] Costa-Fernández, J. M., Rosario Pereiro, and Alfredo Sanz-Medel. "The Use of Luminescent Quantum Dots for Optical Sensing." *TrAC Trends in Analytical Chemistry* 25.3 (2006): 207-18.

[10] Bruchez, M., M. Moronne, P. Gin, S. Weiss, and A. Alivisatos. "Semiconductor nanocrystals as fluorescent labels." *Science* 281 (1998): 2013-2016.

[11] Hild, W., M. Breunig, and A. Goepferich. "Quantum Dots - Nano-sized Probes for the Exploration of Cellular and Intracellular Targeting." *Europ. J. of Pharm. and Biopharm.* 68 (2008): 153-68.

[12]Jaiswal, J., H Mattoussi, J. Mauro, and S. Simon. "Long-term multiple color imaging of live cells using quantum dots bioconjugates." *Nat. Biotechnol.* 21 (2003): 47-51.

[13]Sutter, J., D. Birch, and O. Rolinski. "The Effect of Intensity of Excitation on CdSe/ZnS Quantum Dots." *Applied Physics Letters* 98 (2011): 21108.

[14] Liu, Y/-S., Y. Sun, T. Vernier, C.-H. Liang, S. Chong, and M. Gundersen. "pH-sensitive Photoluminescence of CdSe/ZnSe/ZnS Quantum Dots in Human Ovarian Cancer Cells." *J. Phys. Chem. C* 111.7 (2007): 2872-2878.

[15] Vega, L., J. Doudal, T. Torchynska, R. Penna Sierra, and L. Shcherbyna. "Transformation of Photoluminescence Spectra at the Bioconjugation of Core-shell CdSe/ZnS Quantum Dots." *Phys. Status Solidi C* 7.3-4 (2010):724-727.

[16] Baù, L., Paolo Tecilla, and Fabrizio Mancin. "Sensing with Fluorescent Nanoparticles." *Nanoscale* 3 (2011): 121-124.

[17] Resch-Genger, U., Markus Grabolle, Sara Cavaliere-Jaricot, Roland Nitschke, and Thomas Nann. "Quantum Dots versus Organic Dyes as Fluorescent Labels." *Nature Methods* 5.9 (2008): 763-775.

[18] "Qdot Nanocrystals technology Overview". *Invitrogen by Life Technologies*. Web.

[19] Huang, Chaobiao, C. Wu, and Y. Zhao. "Extracting fluorescence signal due to direct excitation of the energy acceptor from quantum dot-based FRET." *J. Nanoport Res.* 12 (2010): 2153-2161.

[20] Nic, M., Jiri Jirat, and Bedrich Kosata. *IUPAC goldbook* . Prague: ICT Press, 2006.

[21] Jorge, P., M. Martins, T. Trindado, J. Santos, and F. Farahi. "Optical fiber sensing using quantum dots." *Sensors* 7 (2007): 3489-3534.

[22] Wang, Xiaojuan, C. Boschetti, M. Ruedas-Rama, A. Tunnacliffe, and E. Hall. "Ratiometric pH-dot ANSor." *Analyst* 135 (2010): 1585-1591.

[23] Wang, Y., H. Mao, and L. Wong. "Na+-sensing quantum dots for cell-based screening of intracellular Na+ concentrations." *Talanta* 85 (2010): 694-700.

[24] Tohda, K., H. Lu, Y. Umezawa, and M. Gratzl. "Optical detection in microscopic domains. 2. Inner filter effects for monitoring nonfluorscent molecules with fluorescence." *Anal. Chem.* 73 (2001): 2070-2077.

[25] Dubach, J. M., D. Harjes, and H. Clark. "Ion-Selective Nano-optodes Incorporating Quantum Dots." *JACS* 129 (2007): 8418-8419.

[26] Ruedas-Rama, M., A. Orte, E. Hall, J. Alvarez-Peza, and E. Talaveraa. "Quantum Dot Photoluminescence Lifetime-based PH Nanosensor." *Chem. Commun.* 47 (2011): 2898-900.

[27] Xu, Chao, and Eric Bakker. "Multicolor quantum dot encoding for polymeric particle-based optical ion sensors." *Anal. Chem.* 79 (2007): 3716-3723.

[28] Kumar, Challa S., ed. Microfluidic Devices in Nanotechnology. Hoboken, NJ: Wiley, 2010.

[29] Janasek, D., Joachim Franzke, and Andreas Manz. "Scaling and the Design of Miniaturized Chemical-analysis Systems." *Nature* 442.7101 (2006): 374-80.

[30]Johnson, D., V. Gavalas, S. Daunert, and L. Bachas. "Microfluidic ion-sensing devices." *Anal. Chim. Acta* 613 (2008): 20-30.

[31] Becker, H., and Claudia Gartner. "Polymer microfabrication methods for microfluidic analytical applications." *Electrophoresis* 21 (2000): 12-26.

[32] Whitesides, G. M. "The Origins and the Future of Microfluidics." *Nature* 442.7101 (2006): 368-73

[33] Mair, D., E. Geiger, A. Pisano, J. Frechet, and F. Svec. "Injection Molded Microfluidic Chips Featuring Integrated Interconnects." *Lab on a Chip* 6 (2006): 1346-354.

[34] Tsao, Chia-Wen, and Don DeVoe. "Bonding of thermoplastic polymer microfluidics." *Microfluid. Nanofluid.* 6 (2009): 1-16.

[35] Heckele. M., Schomburg W . “Review on micromolding of thermoplastic polymers”. *J. Micromech. Microeng.* 14 (2004): 1-4.

[36] Leech, P. W. "Hot Embossing of Cyclic Olefin Copolymers." *J.Micromech. Microeng.* 19.5 (2009): 055008.

[37] Koesdjojo, M., Y. Tennico, and V. Remcho. "Fabrication of microfluidic system for capillary electrophoresis using a two-stage embossing technique and solvent welding on poly(methyl methacrylate) with water as a sacrificial layer." *Anal. Chem.* 80 (2008): 2311-2318.

[38] Becker, Holger, C. Gartner. "Polymer microfabrication technologies for microfluidic systems." *Anal. Bioanal.Chem*. 390 (2008): 89-111.

[39] Rainelli, A,, R. Stratz, K. Schweizer, and P. Hauser. "Miniature flow-injection analysis manifold created by micromilling." *Talanta* 61 (2003): 659-665.

[40] Pan, C., H. Yang, S. Shen, M. Chou, and H. Chou. "A low-temperature wafer bonding technique using patternable materials ." *J. Micromech. Microeng.* 12 (2002): 611-615.

[41] Tsao C., Hromada L., Liu J., Kumar P., deVoe D. "Low temperature bonding of PMMA and COC microfluidic substrates using UV/ozone surface treatment". *Lab on Chip* 7 (2007): 499-505.

[42] Tennico, Yolanda H., Myra T. Koesdjojo, Saki Kondo, David T. Mandrell, and Vincent Remcho. "Surface Modification-assisted Bonding of Polymer-based Microfluidic Devices." *Sensors and Actuators B: Chemical* (2009): 799-804.

[43] Kricka, Larry J., Paolo Fortina, Nicholas J. Panaro, Peter Wilding, Goretty Alonso-Amigo, and Holger Becker. "Fabrication of Plastic Microchips by Hot Embossing." *Lab on a Chip* 2.1 (2002): 1-4.

CHAPTER 2

IMPROVEMENT IN RESPONSE OF ION-SELECTIVE OPTICAL SENSORS

2.1. Introduction

As described in chapter 1, ion-selective optical sensors (ISOs or optodes) are nano/microparticles specifically designed for the intracellular monitoring of small analytes (ions).

Typically, a regular cation-selective optode contains an ionophore that selectively binds a target ion (cation) and a second ionophore (chromoionophore) that interacts with a reference ion (proton) and changes its optical properties. The response of an ISO is dictated by the ion-exchange equilibrium between the target analyte (and any interferents) and the optode. In more detail, when a cation binds to an ionophore, ion-exchange occurs in order to maintain charge balance. The exchanged cation is ordinarily H+, thus the hydrogen-ion activity inside the sensor decreases which leads to optical changes in the chromoionophore spectrum – the ion exchange process leads to a proportional change in optical signal. The main advantage of ISOs is the fact that all of the sensing components are embedded in a single inert polymer matrix, through which the analyte must diffuse to reach the incorporated organic dye to then trigger the change in optical signal intensity (fluorescence).

The drawback of this kind of sensor is rapid organic dye photobleaching upon excitation (it has been shown that many organic dyes will photobleach in less than a minute [1]). One of the possible alternative approaches by which this problem may be addressed is to excite the dye *indirectly*.

Our research group has successfully fabricated sodium selective ISOs with two main sensing components: sodium ionophore X and organic dye - chromoionophore I (ETH 5294). The latter is a proton-carrier neutral fluorescent dye - a lipophilic isologue of Nile Blue dye [2]. This specific dye has the useful property of shifting its fluorescence intensity maximum in response to changes in pH. In its fully protonated form it has peak at 680 nm, while in its fully deprotonated form the maximum is at 655 nm (Figure 2.1).

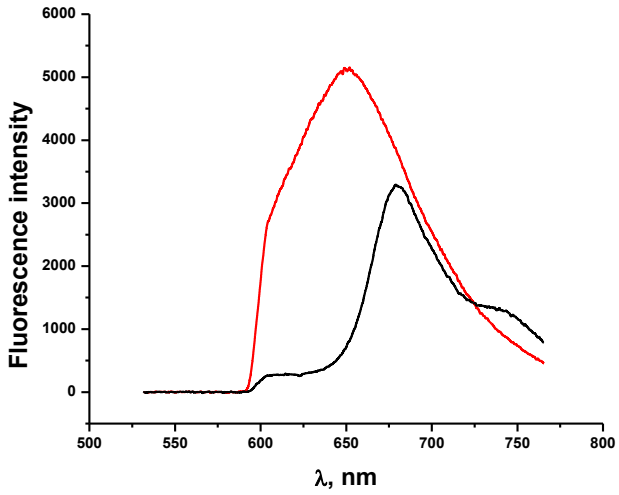

Figure 2.1. Fluorescence spectra of protonated (black) and deprotonated (red) forms of chromoionophore I.

When the dye is partially protonated the maximum lies between 655 and 680 nm. Subject to calibration, the fluorescence intensity can therefore be used as a diagnostic tool for pH determination.

Since the absolute intensity of the fluorescence peak depends on a number of different factors (noise, light intensity fluctuations, quenching and various other solution-dependent phenomena are the principal influences), greater assay integrity can be achieved if measurements are made based on *relative* intensities. For this purpose, ratiometric measurements were introduced in our studies.

Ratiometric measurements minimize the effect of light fluctuations from the source and microenvironment during measurements and help to avoid effects of excitation intensity differences.

Thus, α - a mole fraction of unprotonated chromoionophore - is used as the sensor's response function and calculated according to the formula below (Equations. 2.1, 2.2).

$$\alpha = \frac{F_{pr} - F}{F_{pr} - F_{dpr}} \quad \text{(Equation 2.1)}$$

$$F = \frac{(fluorescence\ intensity\ of\ peak\ at\ 655\ nm)}{(fluorescence\ intensity\ of\ peak\ at\ 680\ nm)} = \frac{I_{655}}{I_{680}} \quad \text{(Equation 2.2)}$$

where 655 nm and 680 nm are peak maximum positions of the deprotonated and protonated forms of choromoionophore I respectively;

F is a fluorescence intensities ratio measured in the current experiment;

F_{pr} and F_{dpr} - fluorescence intensities ratios of the fully protonated and fully deprotonated forms of chromoionophore I respectively.

Typically, to excite chromoionophore I an enormous light intensity from a fluorescence microscope light source is used. This causes rapid photobleaching of the dye (as an example, for 200 nm particle, 10-20 seconds of constant illumination was sufficient to cause complete photobleaching of the dye).

The purpose of this study was to overcome the problem of organic dye optical degradation by introducing an additional fluorescent component to the optode matrix - quantum dots (QDs) that are well-known for their extreme resistivity to photobleaching.

The approach used in this project is to add QDs to the polymer matrix and then, instead of direct excitation of chromoionophore I, to excite QDs in the near UV region where the dye has no absorbance (Figure 2.2.).

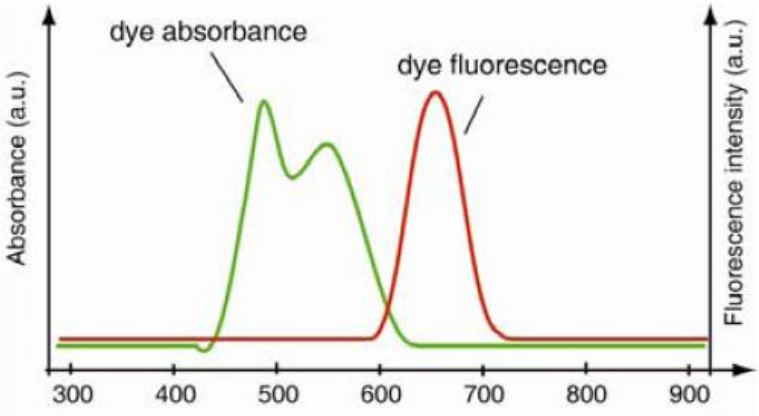

Figure 2.2. Approximate absorption and emission spectra of chromoionophore I.

To accomplish this, the emission of QDs would ideally be matched with the absorbance band of chromoionophore I. This is easily achieved owing to the huge variety of QDs with different emission peak positions that are currently available on the market.

Thus, the dye will absorb the energy emitted by the QDs and the inner filter effect will yield a concentration-dependent signal (Figure 2.3). In this case chromoionophore I will work in much "softer" conditions (conditions less likely to result in photobleaching).

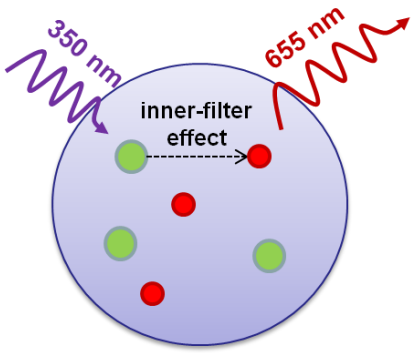

Figure 2.3. Diagram illustrating optode response via the inner filter effect.

This new sensor thus combines the properties of "traditional" ISOs and the inner-filter effect to yield a more effective measurement tool.

To perform a ratiometric measurement, two absorbance bands of chromoionophore I were used and two types of QDs (to match the two absorbance peaks of the dye) were incorporated. This approach allowed for the measurement of emission quenching (caused by the dye) from two separate QDs. Thus, there will be two data points and the possibility to take a ratio which is indicative of the degree of dye protonation (Figure 2.4).

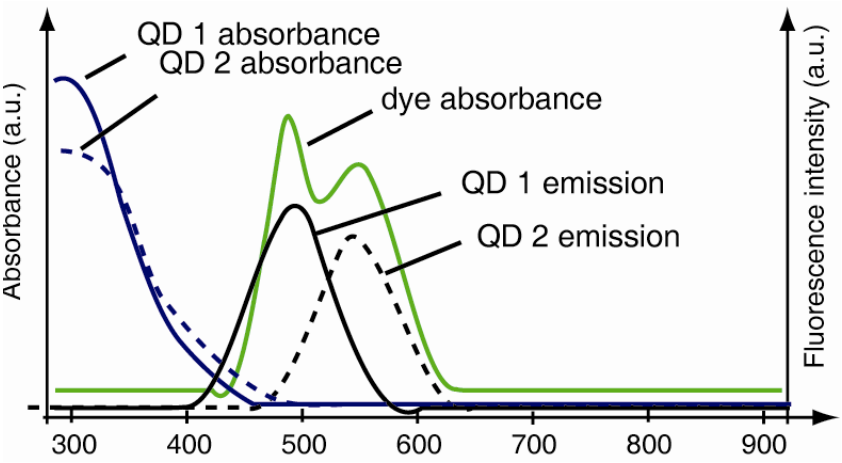

Figure 2.4. Explanation of ISO/QD response based on the inner filter effect.

This means that the response function (α) formula will include a *QD emission peak ratio* instead of the *protonated/deprotonated form ratio* as was described above (Equation 2.3).

$$F = \frac{(fluorescence\ intensity\ of\ QD_{545}\ peak\ at\ 545\ nm)}{(fluorescence\ intensity\ of\ QD_{605}\ peak\ at\ 605\ nm)} = \frac{I_{545}}{I_{605}} \quad \text{(Equation 2.3)}$$

The fluorescence maxima of chromoionophore I were therefore used only as references and were not taken into account for any calculations.

2.2. Experimental

2.2.1. Reagents

9-(diethylamino)-5-octadecanoylimino-5H-benzo[α]phenoxazine (chromoionophore I or ETH 5294), tert-butyl calix[4]arene tetraehyl ester (sodium ionophore X), potassium tetrakis(4-chlorophenyl) borate (KTCPB), high molecular weight poly(vinyl chloride) (PVC), bis(2-ethylhexyl) sebacate (DOS), polyoxyethylene (23) lauryl ether (Brij-35), tetrahydrofuran (THF), cyclohexanone, acetone, ethylene glycol diethyl ether, tris(hydroxymethyl)aminomethane (Tris-buffer) were purchased from Sigma – Aldrich (Milwaukee, WI).

All aqueous solutions were prepared in deionized water (18.2 MΩ cm; Millipore, Milli-Q Water Systems).

Na^+-solutions were prepared by diluting initial 1.0 M NaCl solution.

10 mM Tris-buffer was used to maintain the desired pH.

The core-shell Qdot® 545/605 ITK™ (QDs in this manuscript is used as a general name for "quantum dots", Qdots is a tradename of QDs sold by Invitrogen) quantum dots (1μM solution in decane) were purchased from Invitrogen (Eugene, OR). According to Invitrogen, Qdot 545 is comprised of 4-5 nm diameter spheres (the organic coating adds approximately another 10nm). Qdot 605 has an ellipsoidal form of approximately 5x12 nm (with an additional 10 nm for the organic coating) (Figure 2.5).

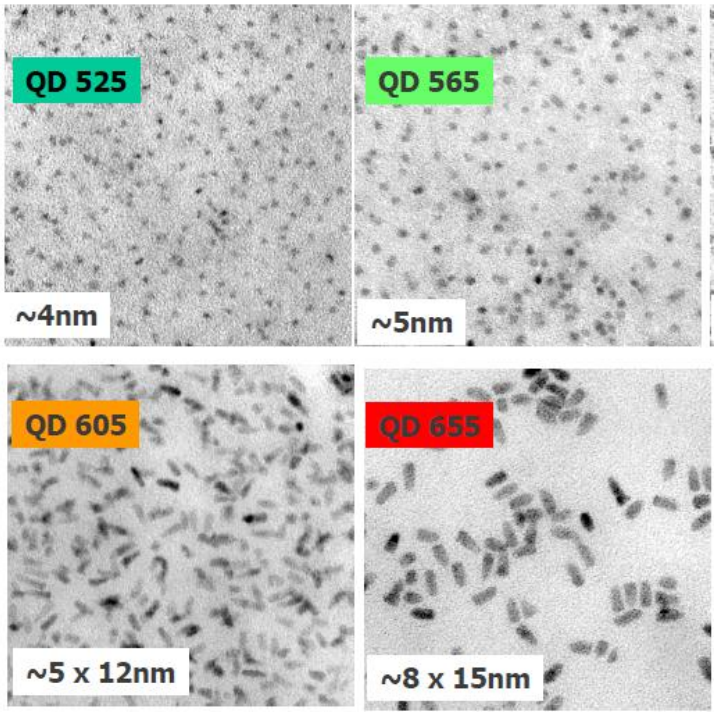

Figure 2.5. TEM images of Qdots (courtesy of Invitrogen, now Life Technologies).

The shipping solvent, decane, in which the QDs were supplied, was displaced with THF in order to avoid the addition of an extra component to the optode synthesis.

2.2.2. Membrane composition

The membrane cocktail contains 10 mmol/[kg of membrane] chromoionophore I (ETH5294), 20 mmol/kg ion-exchanger, 40 mmol/kg sodium ionophore, 15 µmol/kg QD_{545} and 5 µmol/kg QD_{605}. Membranes were made with 33% (w/w) polymer (PVC) and 66% plasticizer (DOS). The active sensor components, polymer and plasticizer (collectively referred to as the "membrane cocktail") were dissolved in 1 mL of cyclohexanone/etyl-glyme (2:1 by volume) solvent mixture and shaken vigorously for 2 hours to achieve homogenity.

Table 2.1. Structural formulas of the components of sodium-selective optode.

Chromoionophore I (ETH 5294)	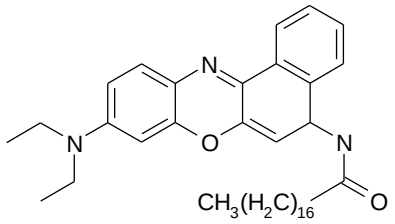
Tert-butyl calix[4]arene tetraehyl ester (sodium ionophore X)	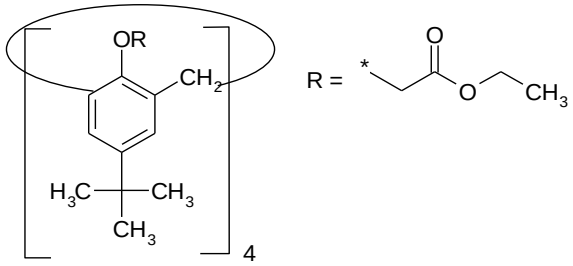
Potassium tetrakis(4-chlorophenyl) borate	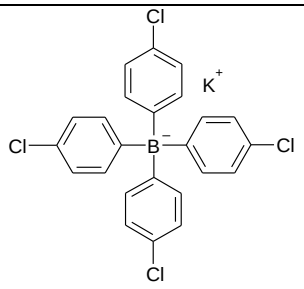

2.2.3. Membrane cocktail preparation.

Core-shell CdSe/ZnS QDs (with emissions at 545 and 605 nm) were blended with sensing components (sodium ionophore X, chromoionophore I, ion-exchanger), PVC matrix and DOS plasticizer in a solvent mixture of cyclohexanone/ethyl-glyme (2:1 by volume). Cyclohexanone/ethyl-glyme mixture was used as initial solvent due to the fact that cyclohexanone is less volatile than THF. Additionally, ethyl-glyme was utilized to ensure even membrane spreading when working with the spin-coated polymer films

2.2.4. Polymer film preparation.

Preliminary experiments were made on optode membranes in the form of polymer films in order to detect and minimize any potential matrix effects on fluorescent signal. This was quite useful in the proof-of-concept phase of the work because the concentrations of the sensing components in the film were much higher than in the optode particles, facilitating both detection and optimization of the signal.

150 µL QD_{545} and 50 µL QD_{605} (QD_{545}/ QD_{605} always kept as 3:1 by volume) was mixed with 100 µL of the membrane cocktail. A PVC/DOS formulation was chosen based on the considerable difference in hydrophobicity between polymer and the surfactant solution in which the polymer was dispersed (a key requirement). To work with aqueous solution of surfactant, it was necessary for the polymer to be hydrophobic. Moreover, as PVC is a hydrophobic polymer and the QDs have lipophilic coatings, these two were mutually compatible.

Films were prepared by spin-coating 70 µL of the membrane cocktail onto 22x22 mm (square) microscope coverslips.

2.2.5. Synthesis of ion-selective optical sensors.

The solvent displacement method was used for optode fabrication [3]. A small vial (7-8 mL) containing 5 mL of 0.01wt% Brij-35 (surfactant) solution in deionized water was used as a reaction vessel, as in the absence of surfactant larger amounts of coagulum were observed and the emulsion was less stable (aggregation followed by precipitation) over time. 200-500 µL (depending on the desired membrane:THF dilution factor) of the membrane cocktail, dissolved in THF, was rapidly injected into the stirred (at approximately 100 rpm) surfactant solution using a disposable 1mL syringe with the needle held 5-7 mm above the surfactant solution surface inside the vial. Within seconds a milky emulsion was formed together with a small amount of coagulum that was mechanically removed.

2.2.6. Optics

An inverted fluorescence microscope (Olympus IX-71, Olympus, Center Valley, PA) interfaced to a Microspec MS-2150 spectrometer (Action Instruments) and PIXIS-512 cooled CCD (charge-coupled device) camera (Princeton Instruments, Trenton, NJ) were used for data collection. A direct imaging CCD camera was also used for spectral imaging to take advantage of the rapid switching capability of its mirror and diffraction grating. The camera and spectrometer were connected to a PC running WinSpec32 software (Princeton Instruments, Trenton, NJ).

A 300W xenon arc lamp (DG-4, Sutter Instruments) with a four-filter fast wavelength switch was used as a light source. The microscope was equipped with a 40x objective (UPlan, Olympus Center Valley, PA).

2.2.7. Spectral recording

Spectra of samples were collected with the 40x objective, using a 500 ms exposure time. A 350±50 nm filter (UV light) for excitation and a 500 nm cut-off filter were employed for wavelength selection in signal recording.

2.2.8. Zeta-potential measurements

Surface ζ-potential of the particles was measured using a ZetaPALS ζ-potential analyzer (Brookheaven Instruments Corporation). Solutions contained 30% (by volume) optode emulsion, 30% 0.01 M NaCl, 10% 0.1 M MOPS/KOH buffer with pH=7.0 in DI water. Final ζ-potential was calculated as the average of three trials with 10 data points each.

2.2.9. Calibration

Polymer films/optode particles were calibrated in two ways: with respect to pH with sodium activity held constant, and with respect to Na^+ activity with pH held constant (in buffered solution).

2.2.10. Calculations

The mole fraction of protonated chromoionophore I (1-α), where α is the mole fraction of unprotonated chromoionophore respectively, was used as the sensor response function and calculated using Equation 2.1. Two emission maxima (545 nm and 605 nm) from QD_{545} and QD_{605} were used to perform ratiometric measurements.

2.2.11. Calibration curves

Calibration curves have a sigmoidal shape and were fitted to experimental data points by adjusting theoretically calculated values for the exchange constant (K_{exch}) between the organic phase (polymer) and the aqueous phase (surfactant solution):

- complex between ionophore *L* and metal ion *I* with charge z^+ ;

- complex between chromoionophore *C* and proton.

For a given system K_{exch} depends on the relative lipophilicities of the metal ion (*I*) with the charge *z* and proton (*H*) (k_I and k_H), the stability constant of the ion-ionophore complex (β_{ILn}), acidity constant (K_a):

$$K_{exch} = \left(\frac{a_H[C]}{[CH^+]}\right)^z \frac{\left[IL_n^{z^+}\right]}{a_I[L]^n} = k_I \beta_{IL_n} \left(\frac{K_a}{k_H}\right)^z \quad \text{(Equation 2.4)}$$

It is also assumed that concentrations in organic phase are proportional to activities.

2.2.12. Limits of detection

Limit of detection and dynamic range were established as the intersections of lines fitted to the linear component of the sigmoidal calibration curve.

2.3. Results

Chromoionophore I (ETH 5294) is lipophilic dye that exists in single-charged protonated form at physiological pH (7-8). The absorbance spectrum of the dye has one peak at 545 nm for the fully deprotonated form and two peaks (605 and 655 nm) for the fully protonated form (Figure 2.6).

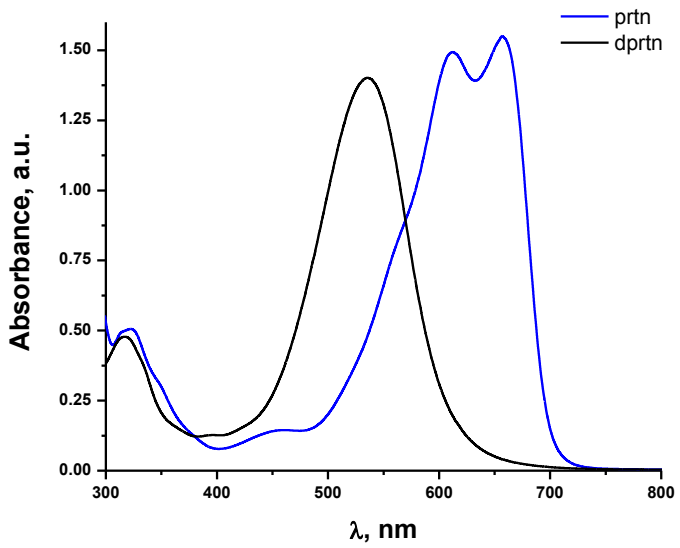

Figure 2.6. Absorbance spectra of protonated (blue) and deprotonated (black) forms of chromoionophore I (ETH5294).

Two types of QDs (with emission maximum at 545 and 605 nm) were purchased from Invitrogen (Figure 2.7) to permit the assembly of the desired ratiometric optode assay system.

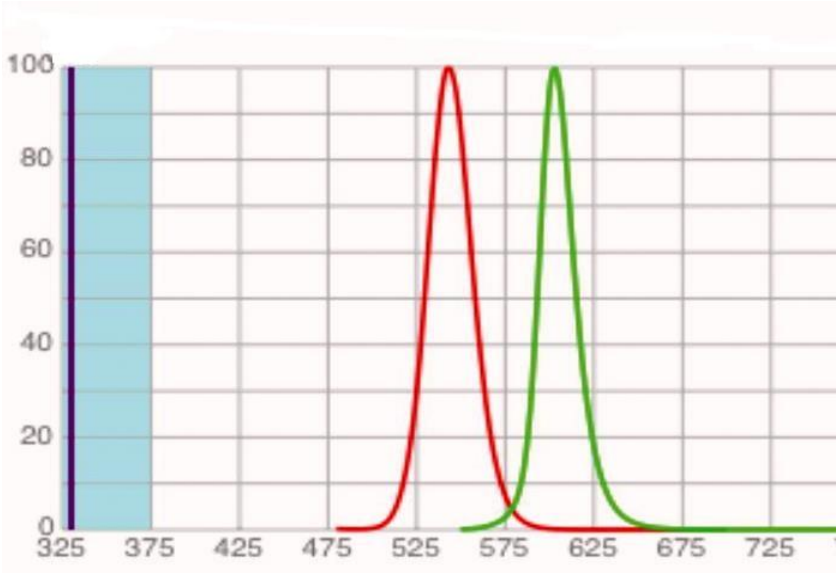

Figure 2.7. Spectra of QD_{545} (red) and QD_{605} (green) generated by Invitrogen's SpectraViewer software.

Invitrogen's Qdots are sold as 1μM solutions in decane. When used as purchased, addition of the QD solution to the membrane cocktail led to the formation of a white precipitate that wasn't observed when the synthesis was done in the absence of the QDs (Figure 2.8).

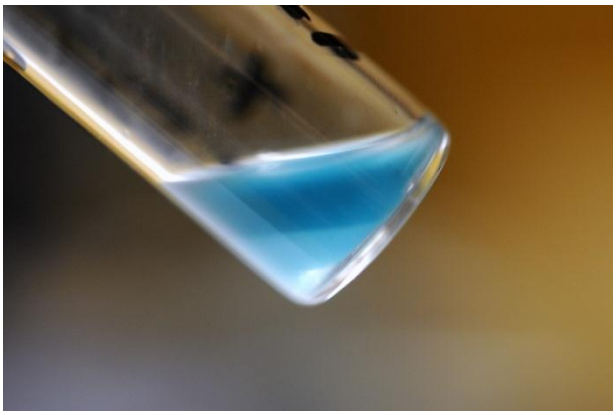

Figure 2.8. White precipitation upon the membrane cocktail addition to QDs in decane.

This undesirable outcome was avoided in future experiments by first performing a solvent-exchange to ensure that the QDs were suspended in THF. Though this sounds simple, the process did require careful attention.

After several unsuccessful attempts to flocculate QDs and resuspend them in THF (as was suggested by the manufacturer), another procedure was developed. Decane was completely evaporated under vacuum, then the QD residue was resuspended in THF. As can be seen on the graph below (Figure 2.9), displacement of decane with THF did not adversely affect the position of the QD emission maxima and bandwidths (differences in peak intensities have a place on the graph because absolute intensities were used). QDs resuspended in THF were therefore utilized for the further experiments.

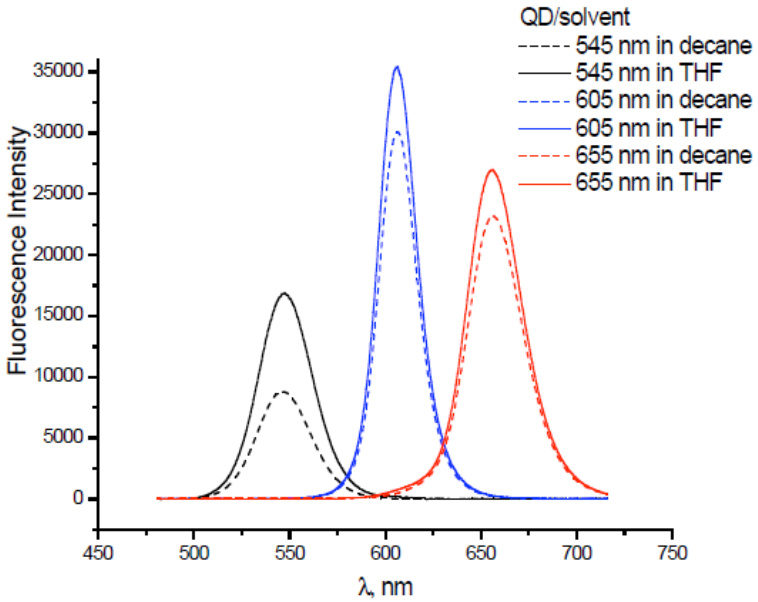

Figure 2.9. Invitrogen ITK organic QDots 545 (black), 605 (blue), 655 (red) in decane (original solvent) and THF (replaced solvent)

As a result of different manipulations, it was noticed that QD nanocrystals are not equally stable across a wide pH range; fluorescence quenching was observed in extremely acidic and basic solutions. The optimum pH for use of the QDs employed in the IFE-based assay was determined experimentally, and is presented on Figure 2.10.

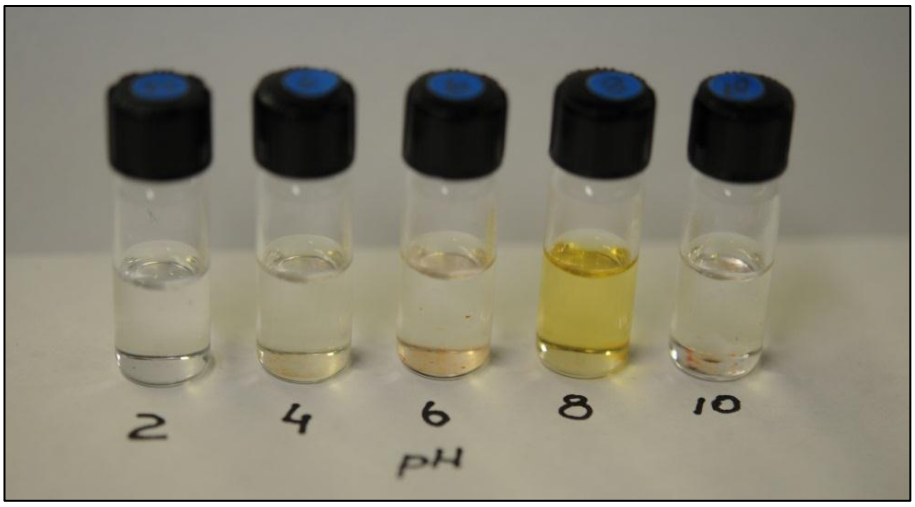

Figure 2.10. Invitrogen's ITK organic Qdots at different pH. It was determined that the QDs perform optimally at near-physiological pH.

As seen above, the "safe" pH-range for experiments that involve QDs is 7- 9.

The proof-of-concept work began with polymer films spin-coated onto microscope cover slips, in which case the concentrations of sensing components were higher making it easier to detect a signal and any changes in signal arising from variations in solution conditions. In support of this effort, a ratiometric determination of signal intensity was performed. As Invitrogen does not indicate the composition of its Qdot coating, and it is hard to predict the chemistry involved in fluorescence quenching at various pH conditions in the absence of this information, QDs in the membrane cocktail were exposed to pH 2-11 solution conditions for 10 min (Figure 2.11).

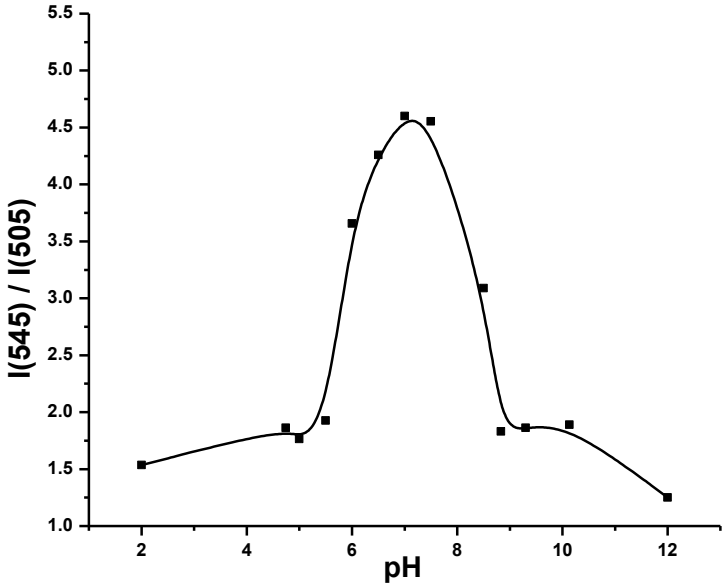

Figure 2.11. pH-dependence of QDs fluorescence (y-axis described intensity ratio of signal from QD_{545} to the background) in optodes membrane prepared as polymer film.

This experiment shows that the QDs selected for these studies were effective signaling tools in solution conditions between pH 6.5 and pH 9.0. This range is ideal for our application, as our ultimate goal is to use optodes in biological matrices where physiological pH is close to the "safe" pH-range for QDs.

An extensive literature search revealed only a few papers that mentioned the pH instability of nanocrystals, though the Invitrogen web-site states that Qdots are designed to work at neutral pH. We hypothesize that possible explanation to this is the following:

under acidic (pH<4) and basic (pH>10) conditions lipophilic coating on the quantum dots hydrolyzes [4]. The lipophilic polymer layer becomes too thin to support the micelle-like structure [5] which causes QDs aggregation with following precipitation.

To demonstrate that chromoionophore I would be excited only by the light emitted by the QDs and not by light from other sources, we collected two spectra (Figure 2.12). Optodes containing chromoionophore and QD_{655} were excited at 350 nm (UV) and 535 nm.

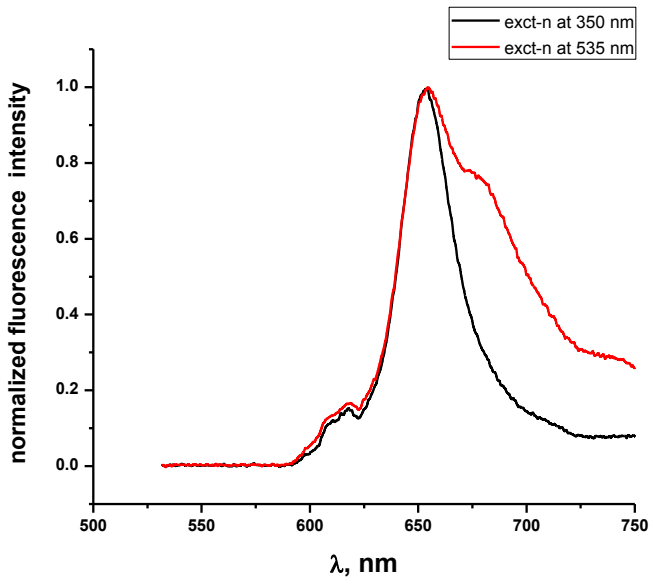

Figure 2.12 . Fluorescence spectra of optodes that contain chromoionophore I and QD_{655} upon excitation at 350 nm (red line) and 535 nm (black); pH=7.

We conclude that, as predicted, chromoionophore I is not excited by the UV-light (no peak at 680 nm after excitation at 350 nm), while when excited at 535 nm a peak for protonated form of the dye is clearly seen. Thus, if the optodes are excited with UV-light, no adverse signal is seen: chromoionophore I was excited only by the QD emission (the desired inner filter effect).

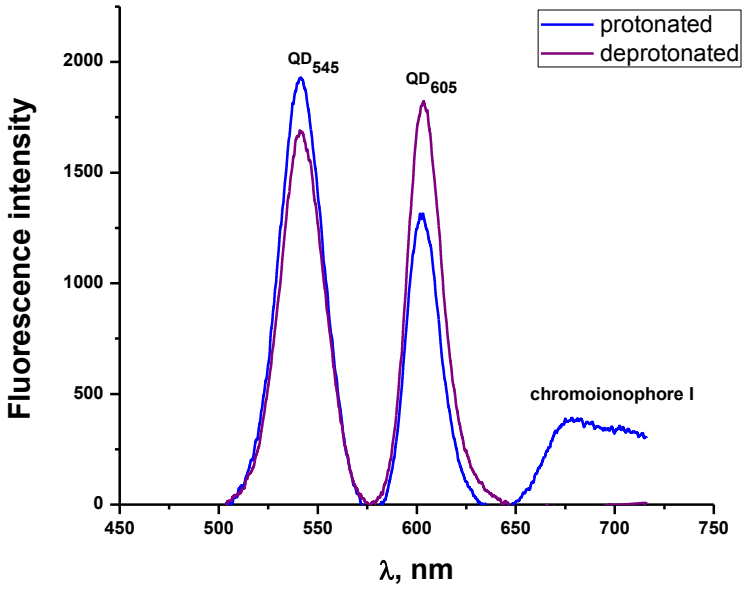

Figure 2.13. Fluorescence spectra of optode membrane as a polymer film at pH=6.0 (purple) and pH=9.0 (blue)

As expected, the polymer film responded to changes in solution pH under conditions of constant activity of the primary metal-ion (Figure 2.13). At pH 6.5 chromoionophore I exists in its protonated form and fluorescence of QD_{605} is quenched, indicating that the inner-filter effect is responsible for the excitation of the protonated form of the dye. The "tail" in the spectrum of protonated form is positioned in such a way that its maximum is at 680 nm; this is coincident with the expected peak maximum for chromoionophore I in the absence of QDs. At pH 9.0, chromoionophore I exists in its protonated form; the fluorescence of QD_{545} is reduced indicating that the inner-filter effect is responsible for the excitation of the deprotonated form of the dye.

After evaluating the behavior of the QDs in the polymeric matrix, we fabricated ion-optodes as microsphere sensor particles via the solvent displacement method (Figure 2.14).

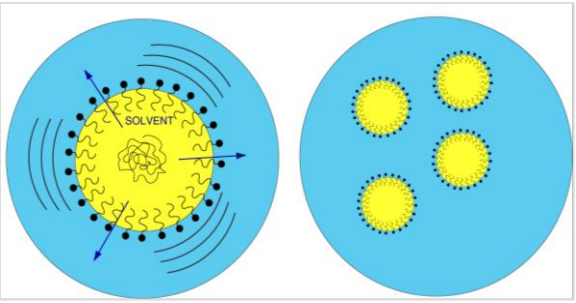

Figure 2.14. The solvent displacement method leads to the production of uniform optode microspheres.

As was mentioned before, the primary advantage of this technique is that all of the required sensing components are dissolved in the same polymer matrix. The key contribution to the science of ion optodes arising from this research effort is the use of QDs to harness the inner filter effect to achieve greater selectivity and sensitivity. Optode synthesis consists of two steps. First, the previously described membrane cocktail (PVC, DOS, Na^+-ionophore, chromoionophore I, KTCPB and QDs selected as appropriate to the particular sensing need) was mixed with the water-miscible solvent - THF. Next, the polymer solution was rapidly injected into the stirred surfactant solution (0.01 % wt. Brij-35), allowing the solvent to diffuse into the aqueous phase. This led to particle precipitation and, thus, a milky solution of ready-to-use optode particles (Figure 2.15).

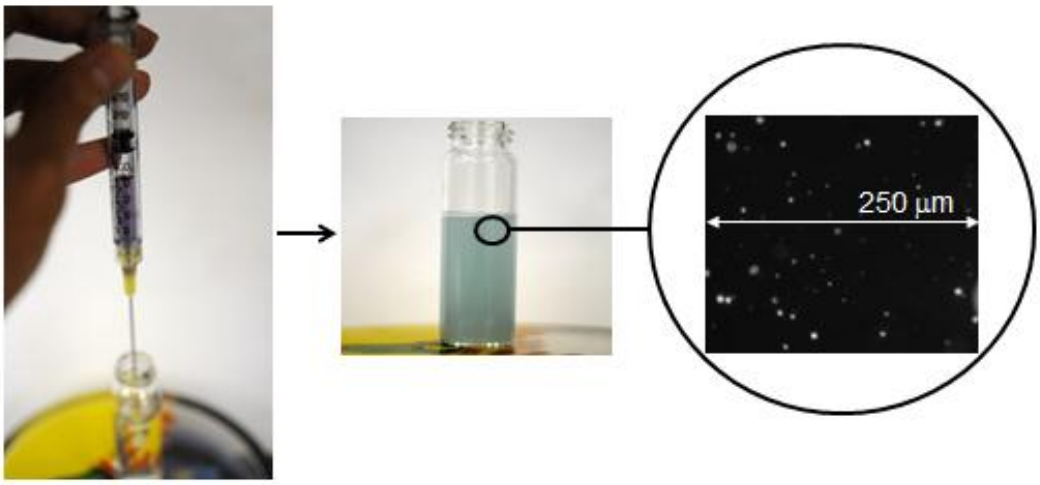

Figure 2.15. Pictorial representation of optode synthesis by the solvent displacement method.

Surprisingly, when the sample-solution pH-dependence of the optodes was probed, it was determined that the QDs were *more* stable than those incorporated in the membrane prepared as a polymer film (Figure 2.16).

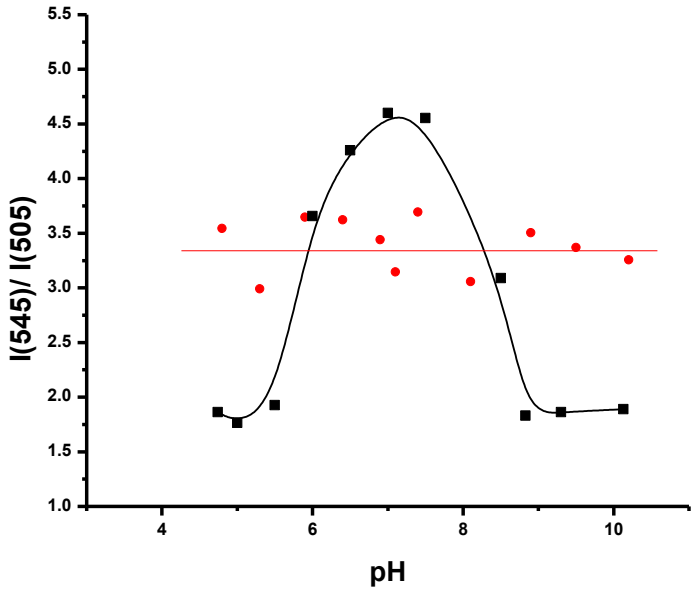

Figure 2.16. pH-dependence of QDs fluorescence optodes' membrane prepared as a polymer film (black) and spherical particles (red).

Our hypothesis is that the polymer membrane is perhaps more impervious in the microparticulate formulation than in the membrane formulation, and thus it serves as a protective barrier for the QDs. Moreover, optodes in the form of spherical particles contain molecules of surfactant that are concentrated on the surface of the particle and have long hydrophobic "tails" which may additionally play a protective role.

The ζ-potential of the optodes (the potential drop across the charged double-layer at the surface of the QD-containing particles) was measured in order to determine the stability of optode emulsion. The magnitude and stability-over-time of this parameter provides information about stability of the colloidal system. Without QDs, the "optodes" were stable with ζ-potential (- 55 ± 5) mV. After incorporation of the QDs into the optodes, the ζ-potential changed to (- 53 ± 4) mV. This very slight change (if we take errors into account two values may be even equal) indicates that the QD-containing optodes still form a stable emulsion.

The response time of the optodes was estimated by taking consecutive spectra of the sample. It was determined that the optodes respond with remarkable speed, essentially instantaneously. The optodes were then tested to determine their utility as pH sensors in the working range of pH 6-9.

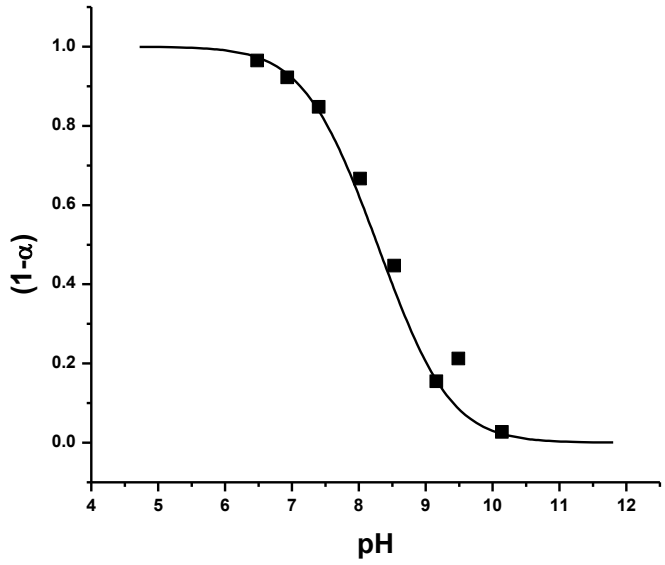

Figure 2.17. Calibration of polymer films with the respect to pH (1 mM Na^+).

The resulting S-shaped curve provided a linear response (dynamic range) from pH 7.1 to 9.5 (Figure 2.17). This working range suggests that the optodes are suitable for use in physiological measurements. At 1 mM Na^+ constant presence, the lower detection limit for the proposed optodes is pH=7.1.

The same batch of optodes was then tested to determine their utility in determining sodium activity (Figure 2.18). This time the sample solution was buffered with TRIS-buffer at pH=7.5 (H^+ concentration was kept constant).

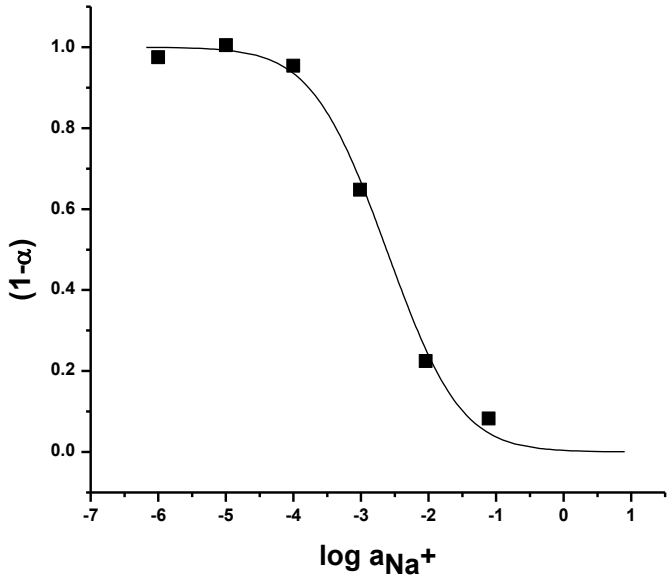

Figure 2.18. Calibration of polymer films with the respect to Na^+ activity; pH=7.5.

The sodium optode detection limit estimated from the graph above, at pH=7.5, is $5x10^{-4}$ M with a dynamic range of ($5x10^{-4}$) – ($5x10^{-1}$) M.

Both the pH and p[Na+] calibration curves are in a good agreement with the theoretical predictions (indicated as lines on Figures 2.17 and 2.18).

Since our QD-based optodes contain the same sensing components as regular ion-selective optodes, we can consider that the selectivity of such sensors remains the same as of ISO. The latter was extensively studied by our research group and described in papers [3,6] which were published previously.

2.4. Conclusion.

Semiconductor nanocrystalls (quantum dots) due to their high resistivity to photobleaching, can be used in ion-selective optodes as excitation donors for inner filter effect based sensors in concert with organic dyes as acceptors. It was determined that QDs are extremely sensitive to hydrolysis in acidic and basic solutions, and therefore they should be used only in neutral media. This is not a significant limitation with optodes such as these which are intended for use in biological systems, as physiological pH is close to neutral.

QDs were incorporated into the polymer matrix along with all of the required sensing components and were excited in the UV-region where the chosen organic dye sensor component exhibits no appreciable absorbance. Upon QD fluorescence the dye is excited and the response of the optodes is measured indirectly as the extent of QD fluorescence quenching that corresponds to the mole fraction of protonated/deprotonated dye in the sample.

It was shown that these optodes respond well as both pH- and sodium-ion sensors.

2.5. References.

[1] Boldt, K., Oliver T. Bruns, Nikolai Gaponik, and Alexander Eychmüller. "Comparative Examination of the Stability of Semiconductor Quantum Dots in Various Biochemical Buffers." *The Journal of Physical Chemistry B* 110.5 (2006): 1959-963.

[2] Morf, W. E., Kurt. Seiler, Bruno. Rusterholz, and Wilhelm. Simon. "Design of a Novel Calcium-selective Optode Membrane Based on Neutral Ionophores." *Analytical Chemistry* 62.7 (1990): 738-42.

[3]Bychkova, V., and A. Shvarev. "Fabrication of micrometer and submicrometer-sized ion-selective optodes via a solvent displacement process." *Anal. Chem* 81 (2009): 2325-2331.

[4] Dra, S., H. Ngzhu, V. Colvin, and P. Alvarez. "Quantum Dots Weathering Results in Microbial Toxicity." *Environ. Sci. Technol.* 42 (2008): 9424-430.

[5] Aldana, J., Y. Andrew Wang, and Xiaogang Peng. "Photochemical Instability of CdSe Nanocrystals Coated by Hydrophilic Thiols." *JACS* (2006): 345-354.

[6] Bychkova, V., and A. Shvarev. "Surface Area Effects on the Response Mechanism of Ion Optodes: A Preliminary Study." *Anal. Chem* 81 (2009): 7416-7420.

CHAPTER 3

IMPROVEMENT IN SYNTHESIS OF ION-SELECTIVE OPTICAL SENSORS

3.1. Introduction

As indicated in the previous chapter, the solvent displacement method was applied successfully for optode fabrication. The main advantage of this method is the possibility of incorporating all required sensor components (chromoionophore I, ion-exchanger, ionophore, PVC and plasticizer) into a single system to yield a "membrane cocktail". A single-step (batch) process was all that was required to produce microparticulate optodes. This process involved injection of the membrane cocktail (dissolved in an organic solvent miscible with water) into an aqueous solution of surfactant (Brij-35). A small amount of polymer solution was rapidly injected into a stirred surfactant solution. Almost instantly, precipitation and formation of an emulsion was observed.

The type of solvent played an important role in production of particles of a certain diameter (Figure 3.1).

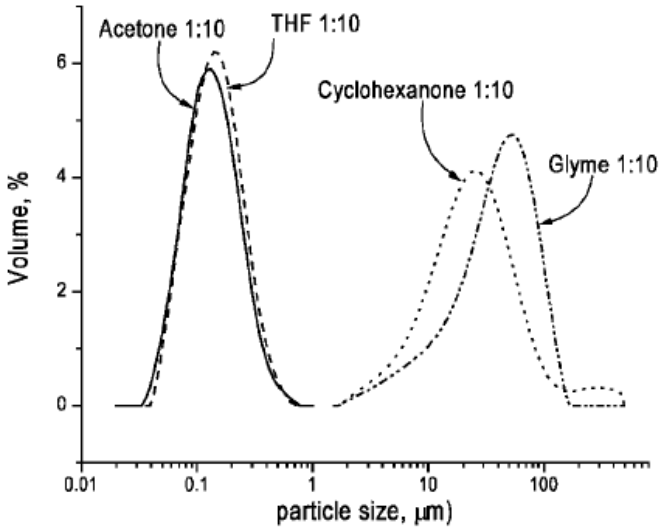

Figure 3.1. Particle size dependence on the type of polymer used for the synthesis [1].

It was shown that if cyclohexanone or ethyl-glyme was used to dilute the membrane cocktail at a ratio of 1:10 (one part membrane cocktail to ten parts solvent by volume) the average size of the resultant particles was 50 μm and 25 μm for cyclohexanone and glyme, respectively. Since the main purpose in producing the optodes is to use them to probe living cells, these sizes are excessive. Acetone and THF allow the

production of particles in the submicrometer range with an average diameter of 200 nm, which is far superior for intracellular applications. Thus, in order to obtain sub-micron particles, acetone or THF should be used.

By choosing a type of a solvent for the fabrication procedure we can “coarse”-tune the particle size. A “fine”-tuning technique for size selection is to vary the membrane-to-solvent dilution factor (Figure 3.2). As an example, dilution with tetrahydrofuran (THF) was studied more extensively. THF was added to dilute the membrane cocktail in the range from 1:1 (one part cocktail to one part THF by volume) to 1:10. The 1:1 dilution yielded optode particles with an average size of 20 μm, the 1:5 dilution yielded 5 μm particles, and the 1:10 dilution yielded 200 nm particles.

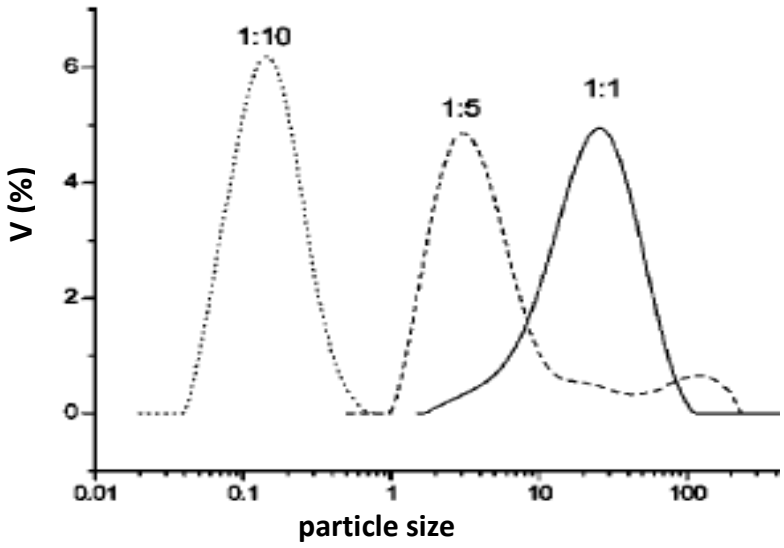

Figure 3.2. Effect of polymer concentration in THF on the size of the particles. The membrane cocktail was diluted to 1:5, 1:10 ratio[1].

The disadvantage of this method is that it is hard to control the mixing process and thus the size and quality of the particles lack reproducibility. In spite of the two possible means for optode size tuning described above, it remains quite challenging to optimize synthetic conditions in the batch mode. Moreover, optodes have relatively short lifetimes and it would be ideal if they could be synthesized on demand, in small quantities, and in the desired size range.

We therefore sought to utilize a microfluidic platform for optode synthesis in order to gain better control over the reaction conditions (by changing flow rates and mixing time) and possibility to produce small amounts of sensors on demand using a single platform.

Searching the literature, we discovered that there were already a couple of successful attempts to use microfluidic channels to produce nanoparticles by the Farokhzad group [2], though they had used different precursors and conditions for the synthesis. There was clearly room for additional work.

3.2. Experimental

3.2.1. Microfluidic platform fabrication

The desired microfluidic platform design was sketched in SolidWorks2008 software (Dassault Systèmes SolidWorks Corp.) for rendering into the substrate, cyclic olefin copolymer (COC).

1 mm thick COC sheet goods (Topas grade 8007, Tg=75^0 C) were purchased from Ticona Corp. (Florence, KY).

9 mm thick polyethylene terephthalate (PET) and 5mm thick polycarbonate (PC) for the fixture were from McMaster-Carr (Aurora, OH).

All the fittings for platform-to-world connections (Female Luer Fitting System, Short Headless SealTight) and polytetrafluoroethylene (PTFE) tubing with 1/16" I.D. were purchased from Upchurch Scientific (IDEX Health & Science LLC; Oak Harbor, WA).

1 mL syringes for reagent delivery were from Hamilton (Reno, NV) and were used with a Harvard Apparatus (Holliston, MA) syringe pump.

0.5 mm thick polycarbonate (PC) and 150 μm thick microscope cover slips for the laser tweezers microfluidic platform were from McMaster-Carr and VWR respectively. Double-sided tape (100 μm thick) was from 3M.

3.2.2. Chemicals for optode synthesis.

9-(diethylamino)-5-octadecanoylimino-5H-benzo[α]phenoxazine (chromoionophore I or ETH 5294), tert-butyl calix[4]arene tetraehyl ester (sodium ionophore X), potassium tetrakis(4-chlorophenyl) borate (KTCPB), high molecular weight poly(vinyl chloride) (PVC), bis(2-ethylhexyl) sebacate (DOS), polyoxyethylene (23) lauryl ether (Brij-35), cyclohexanone, acetone, ethylene glycol diethyl ether were purchased from Sigma – Aldrich (Milwaukee, WI).

All aqueous solutions were prepared in deionized water (18.2 MΩ cm; Millipore, Milli-Q Water Systems).

3.2.3. Size distribution measurements

A Hydro 2000S-AWA 2001 particle size analyzer with Mastersizing 2000 software was used to obtain optode size distribution data. This system measures particle size via the low-angle light scattering (LALS) technique and allows characterization of particles in the 50 nm - 50 µm range. Optode emulsions were collected at the outlet from the microfluidic platform or from the synthesis vessel (for particles synthesized in batch mode), and were directly introduced to the measurement cuvette of the particle size analyzer without any additional sample preparation.

3.3. Results and discussion

3.3.1. Design of the microfluidic platform

The very first step in fabrication of any microfluidic device is design. For particle synthesis, the microfluidic platform was designed to allow close adherence to the optimal parameters identified in the batch method (Figure 3.4).

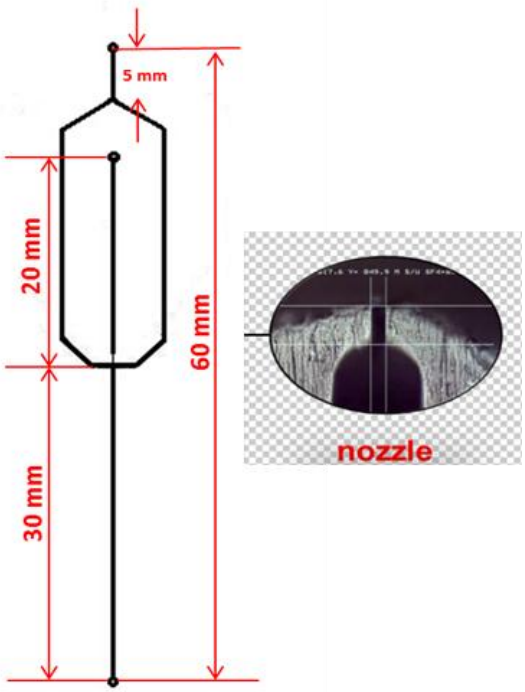

Figure 3.3. Design of proposed microfluidic platform.

In the batch synthesis, a small amount of membrane cocktail was injected into a relatively large volume of surfactant solution via a fine syringe needle. Hence, in order to reproduce the same parameters in the microfluidic design the channels were assembled so as to produce a fine stream of membrane cocktail bounded by the surfactant solution: Using SolidWorks, a 60 mm long x 8 mm device was designed to contain two 30 mm long x 500 μm wide channels (emanating from a single inlet) which would serve as the point of delivery for the aqueous surfactant solution, and a single 20 mm long x 500 μm wide channel (in the middle) with a 60 μm wide nozzle was included for delivery of the organic (membrane cocktail) solution.

All solutions were introduced via two 1 mm (diameter) inlets (one for each solution) and collected from a 1 mm outlet. The aqueous solution stream was split into two streams that were rejoined at the nozzle/outlet junction.

3.3.2. Choice of substrates

The next step in microfluidic device fabrication is substrate (in our case, polymer) selection.

The widely used poly(methyl methacrylate) (PMMA) and polycarbonate (PC) would not have worked for our project's purposes because of their limited resistance to organic solvents (either THF or acetone should be used for the optode syntheses). Polyethylene terephthalate (PET) is resistant to many of the most commonly used organic solvents, but it is very rigid and difficult to process. The optimum choice for solvent displacement synthesis was therefore cyclic olefin copolymer (COC).

COC is a transparent (glass-like) polymer with good chemical resistance. There are only a few companies that produce COC in the US. We selected a COC product from the Ticona Corporation, TOPAS COC, which can be produced with a T_g in the range of 75^0 C to 180^0 C [4].

As was mentioned previously, to produce particles in a narrow (2 μm particle diameter) range the synthesis membrane cocktail must be diluted with either acetone or tetrahydrofuran (THF). Previously, our group worked almost exclusively with THF. Unfortunately, it is rather a challenge to find a polymer that is resistant to THF. COC swells upon contact with THF, but it is perfectly resistant to acetone. Hence, for further experiments, acetone was used for optode fabrication.

3.3.3. Fabrication of the microfluidic platform

The microfluidic platform was fabricated with 1 mm COC (cyclic olefin copolymer; Topas grade 8007, T_g=75^0 C). Two COC plates were cut to the desired size, rinsed with isopropanol and dried with nitrogen prior to processing. Channels (500 μm in depth) were micromilled (Figure 3.5) on two 7.5x3.0 cm COC plates using a high-speed CNC micromill (50,000 rpm spindle).

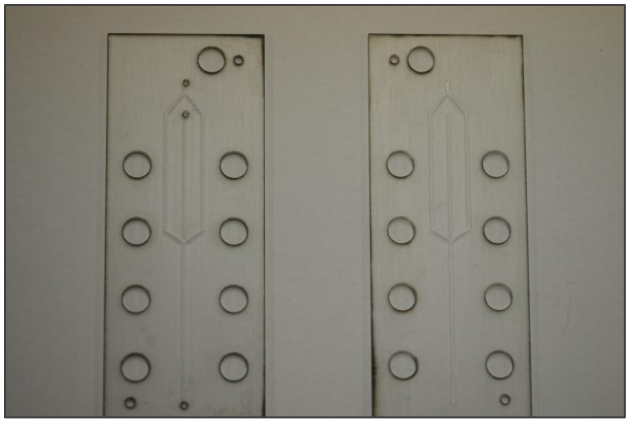

Figure.3.4. Micromilled (on COC) plates of microfluidic platform.

A small nozzle (60 μm wide; previously we tried to work with a 20 μm nozzle, but this proved to be too small and clogged almost instantly) was laser-cut (Figure 3.6) on one COC plate. Inlet/outlet holes (1 mm in diameter) were hand-drilled in the desired location.

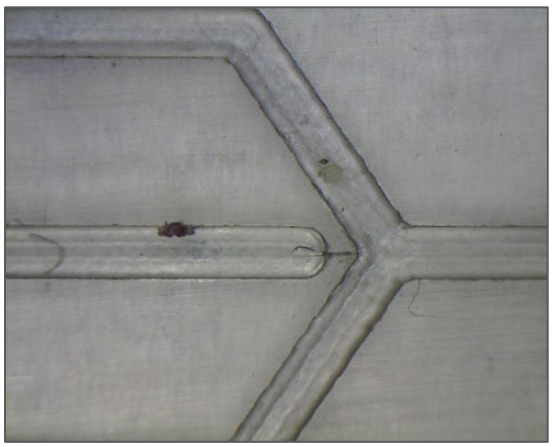

Figure.3.5. Laser-cut 60 μm nozzle.

3.3.4. Bonding method for the microfluidic platform

The microfluidic platform contained a long channel leading to the outlet which was later used for particle trapping, such that very long, straight, fault-intolerant bonding paths were required to ensure a functional device. To achieve this and to ensure solvent

compatibility, it was necessary to avoid conventional bonding methods and instead use an external fixturing approach.

The two COC plates with their micromilled channels were clamped together within an external fixture. Nine threaded holes were drilled on the perimeter of two approximately 1cm thick polymer plates (Figure 3.7). For the bottom plate, polyether terephthalate (PET) was chosen for its good resistivity to organic solvents, while for the top plate polycarbonate (PC) was used owing to its glass-like transparency which allowed for observation of the mixing process.

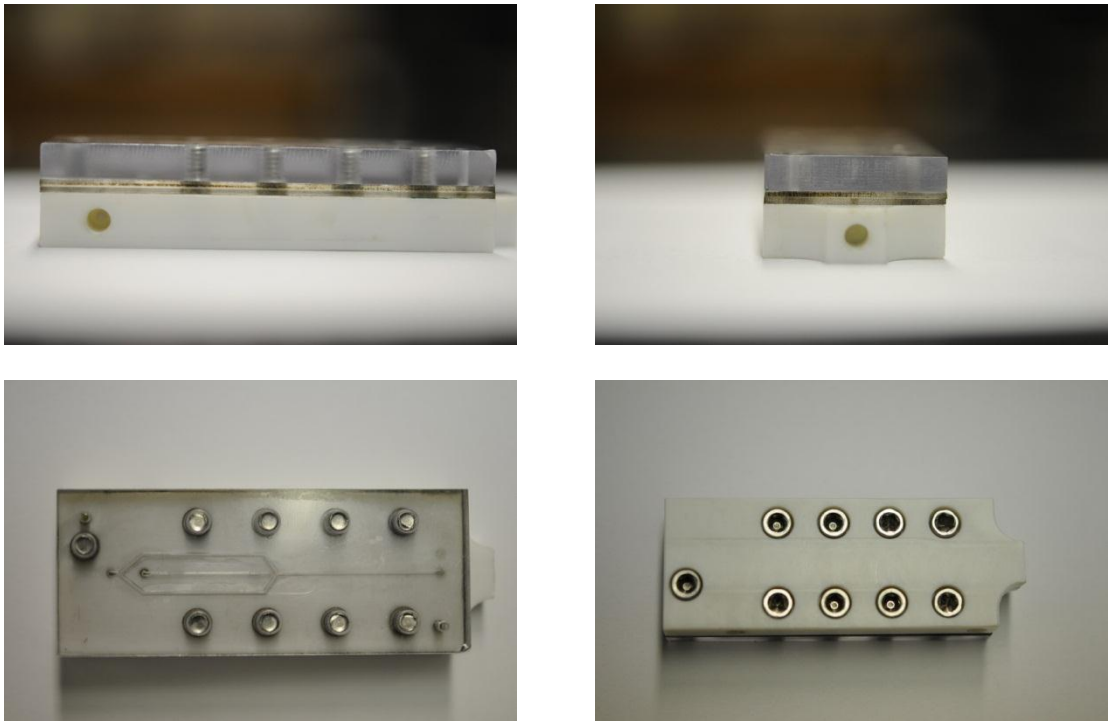

Figure 3.6. PC+PET fixture used for microfluidic platform assembly.

3.3.5. Microfluidic platform-to-world connections.

Solutions were introduced with the help of 1 mL gas-tight syringes mounted on a digitally controlled syringe pump. PTFE tubing with 1/16” I.D. was connected to the syringes and to the threaded inlets in the fixture using commercially-available compression fittings (Upchurch Scientific/IDEX).

3.3.6. Reagents delivery.

A syringe pump was used to deliver both the aqueous surfactant solution and acetone-based membrane cocktail solution (plasticized polymer and sensing components). The two solutions were uniformly mixed in the microreactor, and the particles formed in the reaction were collected at the outlet and analyzed to determine their size distribution using the previously described low angle light scattering tool.

3.3.7. Batch-mode synthesis of optodes

The solvent-displacement method was once again employed for batch-mode optode fabrication [1], this time in acetone rather than in THF. A small vial (7-8 mL) containing 5 mL of 0.01wt% Brij-35 (surfactant) in DI water served as a reaction vessel to which the membrane cocktail solution was added (in the absence of surfactant larger amounts of coagulum were observed and the emulsion was less stable [aggregation followed by precipitation] over time). To this vessel, with rapid stirring, was added 200-500 µL (depending on the desired membrane:acetone dilution factor) of the membrane cocktail. A disposable 1 mL syringe held 5-7 mm above the surfactant solution surface inside the vial was used to dispense the membrane cocktail solution. As had been the case with the THF-based membrane cocktail, within seconds a milky emulsion was formed with a small amount of coagulum that was mechanically removed.

Since previously it was determined that in order to generate the desired nanoparticles the membrane-to-solvent dilution should be less than 1:5, this dilution was chosen as a starting point (Figure 3.8).

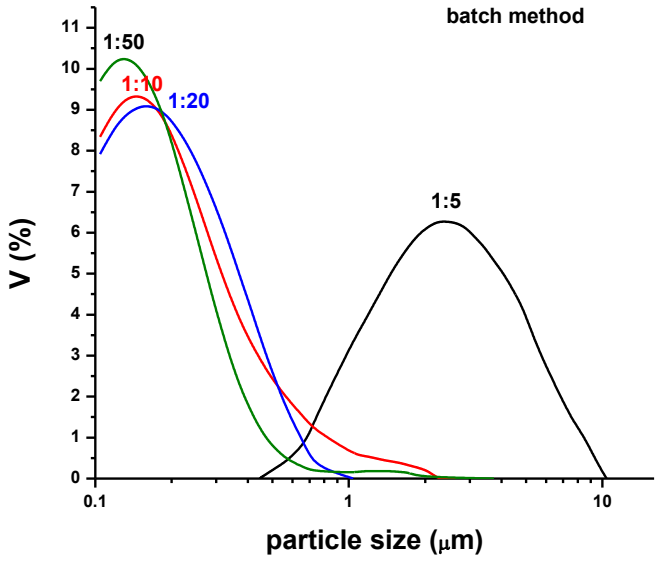

Figure 3.7. Effect of polymer concentration on particle size distribution for optodes synthesized via the batch method in acetone (1:N indicates one part of membrane cocktail to N parts of acetone by volume). Plotted results are an average of ten trials.

As can be seen from the graph, a dilution of 1:5 yielded particles with an average size of 2 μm, while greater dilution factors (1:10 to 1:50) yielded particles in the 100-200 nm range. Thus to generate nanoscale optodes it is necessary to use relatively dilute membrane cocktail solutions.

3.3.8. Synthesis of optodes using the microfluidic platform.

As a proof of concept, synthesis of optodes was performed using a membrane cocktail diluted to 1:10 with acetone in the microfluidic device. Solution compositions were kept the same as in the batch method. Two solutions were mixed inside the microfluidic device at a combined total flow rate of 50 μL/min: 25 μL/min of the aqueous surfactant solution and 25 μL/min of the membrane cocktail solution. The product of the reaction was collected at the outlet and observed under a microscope. As shown in Figure 3.9, spherical particles with an average diameter of 1-3 μm were formed.

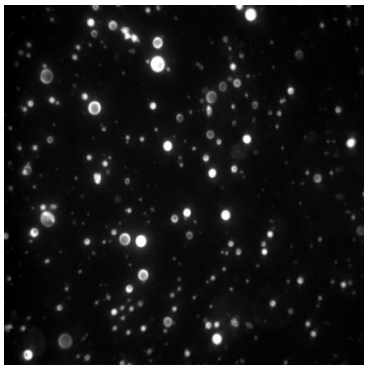

Figure 3.8. Fluorescence images of optodes synthesized using the microfluidic platform.

For all the following experiments, optodes were synthesized in the microfluidic platform by rapid mixing of two solutions: 0.01% aqueous solution of Brij-35 surfactant and organic (acetone) solution of all the sensing components (ionophore, chromoionophore, ion-exchanger in plasticized PVC). Flow rates were controlled using the syringe pump. The resulting optode emulsions were collected at the outlet into 2 mL vials.

To study the effect of membrane cocktail concentration (polymer solution-to-solvent ratio) on the size of optodes, one part (by volume) of the membrane cocktail was diluted with 5-50 parts of acetone (Figure 3.10).

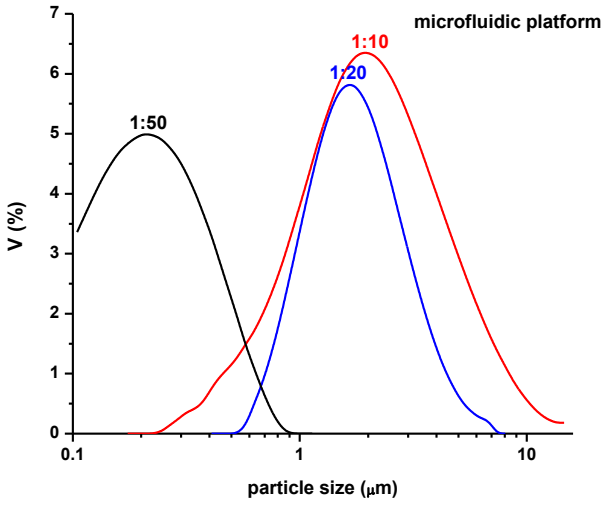

Figure 3.9. Effect of polymer concentration on the size distribution of optodes synthesized in a microfluidic reactor.

It was determined that the optodes synthesized in the microfluidic device exhibited a reasonable degree of monodispersity.

A dilution factor of 1:10 gave particles with average diameter 2 μm, somewhat smaller particles were collected when the dilution was 1:20 and, finally, nano-particles (200 nm) were obtained with a 1:50 dilution. Obviously, when the polymer concentration decreased, the diameter of the particles also decreased.

A dilution of 1:5 produced particles big enough to clog the nozzle within only a few minutes, such that it was impossible to collect enough sample for LALS analysis. No particles were visible if dilution factor was higher than 1:50 (more solvent). Taking into consideration that the lowest particle size that can be detected by LALS method and available equipment is 50 nm, it can be stated that particles with the average diameter bigger than 50 nm can be formed in microfluidic channels only if membrane cocktail is diluted with acetone not more than 1 to 50.

Comparing the size of the particles synthesized by two different methods (Figure 3.11) it is clearly seen that with microfluidic platform the particles are bigger in diameter (here should be taken into account the fact that with 1:5 dilution and microfluidic method particles were big enough to clog the channel) than with batch synthesis (the only exception is dilution 1:50).

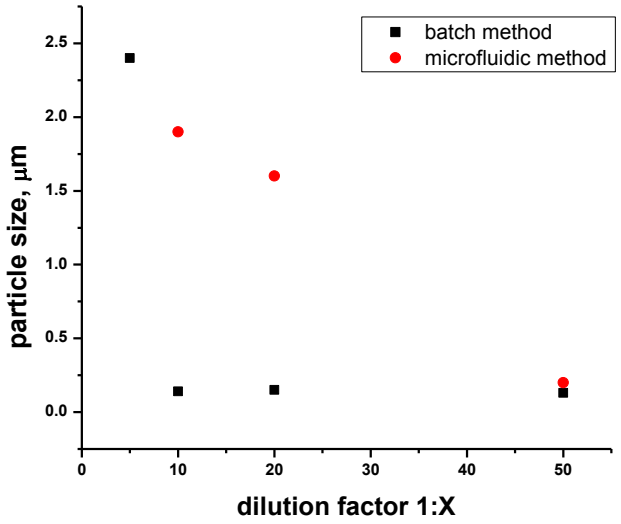

Figure 3.10. Comparison of the effects of the polymer concentration in acetone on the size distribution of optodes synthesized by batch and microfluidics methods.

Since two solutions were delivered via the syringe pump, the particle size dependence on the flow rate ratio was checked. As can be seen from the graph below, there is no such dependence (Figure 3.12 and 3.13). This is not surprising as all of the flow rates studied fell within a region of velocities at which laminar flow occurs: no enhancement in mixing due to turbulent flow is expected. A dilution of 1:50 was used and with every change in the flow rate ratio the size of the particles remained approximately the same (close to 200 nm).

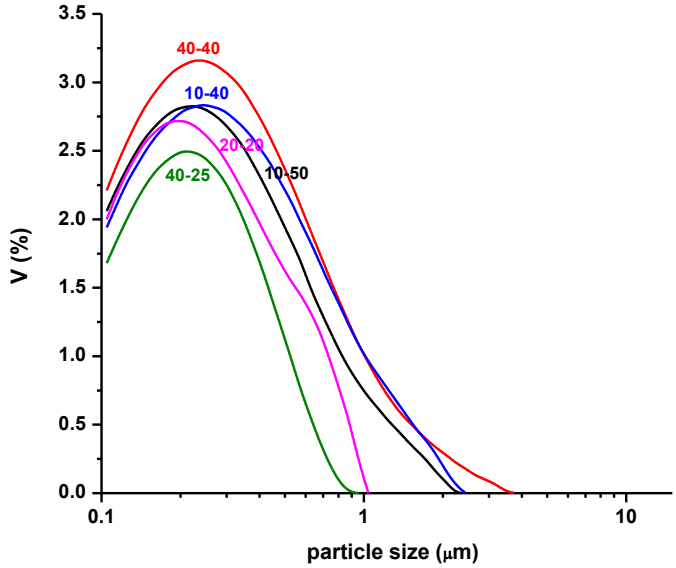

Figure 3.11. Particle size dependence on a flow rate ratio.

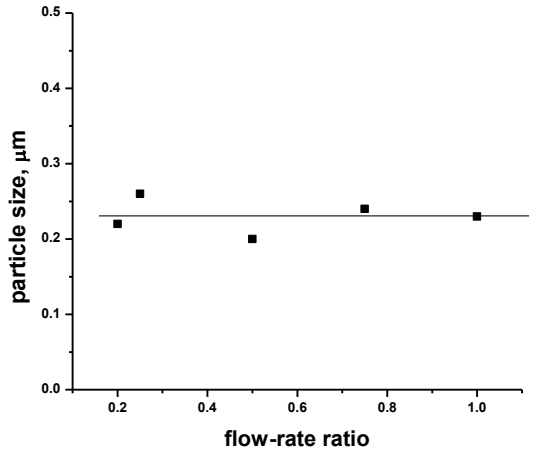

Figure 3.12. Effect of the flow rate ratio on the size distribution of optodes synthesized by batch and microfluidics method.

Hence, particle size has no dependence on the flow rate ratio of reactant solutions and it is safe to work with the fastest flow rates that chosen microfluidic platform can withstand at the same time avoiding backpressure.

3.3.9. Fabrication of the microfluidic platform for laser tweezers trapping.

As was mentioned earlier in this chapter, an additional problem common to experiments with optodes is the difficulty of collecting fluorescence signals due to rapid Brownian motion of the particles in the imaging field. One possible means by which to overcome this problem is to utilize optical tweezers to localize the sensors during the measurement period. This is a separate part of the project that was conducted in collaboration with the McIntyre group in the Department of Physics at OSU.

The idea was to measure optode response immediately after synthesis using optical (laser) tweezers (Figure 3.14).

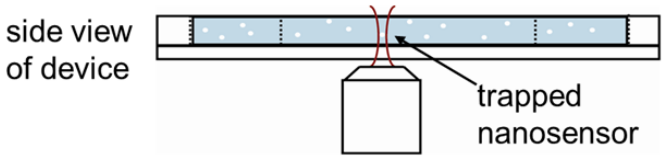

Figure 3.13. Explanation of particle trapping by laser tweezers.

In a field of ion-selective sensors, optical tweezers have mostly been applied to move nano- or microparticles to a given imaging area for more detailed visual studies or specific calibration [3]. A strong focused laser beam exerts a force (from reflected and refracted rays) on a particle that attracts the particle toward the focus where the intensity is the largest. In our system, the goal was to trap the particles within the channel and inject them into a cell (also constrained within the channel) using the trapping laser to perforate the cell membrane.

Thus, it would be ideal to have another microfluidic platform of exceedingly simple design for particle trapping, and couple it directly to the downstream of the platform used for synthesis via teflon tubing of a short length (Figure 3.15).

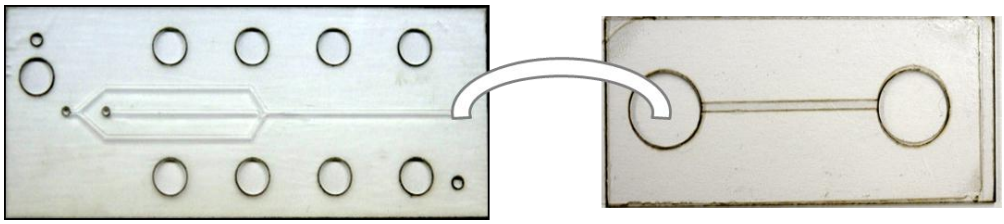

Figure 3.14. Microfluidic platform design for on-line trapping of the optodes after the synthesis process.

Since the particles are dispersed in aqueous solution of surfactant, any polymer that is easy to process may be utilized as a substrate for production of the trapping platform. Thus, one of the easiest option is to make a platform with a 150 μm thick 24x55 mm (hence, the final platform will have the same (width)x(length) dimensions) glass cover slip as lower plate (to facilitate easier laser manipulation of particles) and a polycarbonate upper cover plate (any other polymer could work as well) for simplicity and durability. The two parts of the platform were bonded with 100 μm thick adhesive double-sided tape (Figure 3.16).

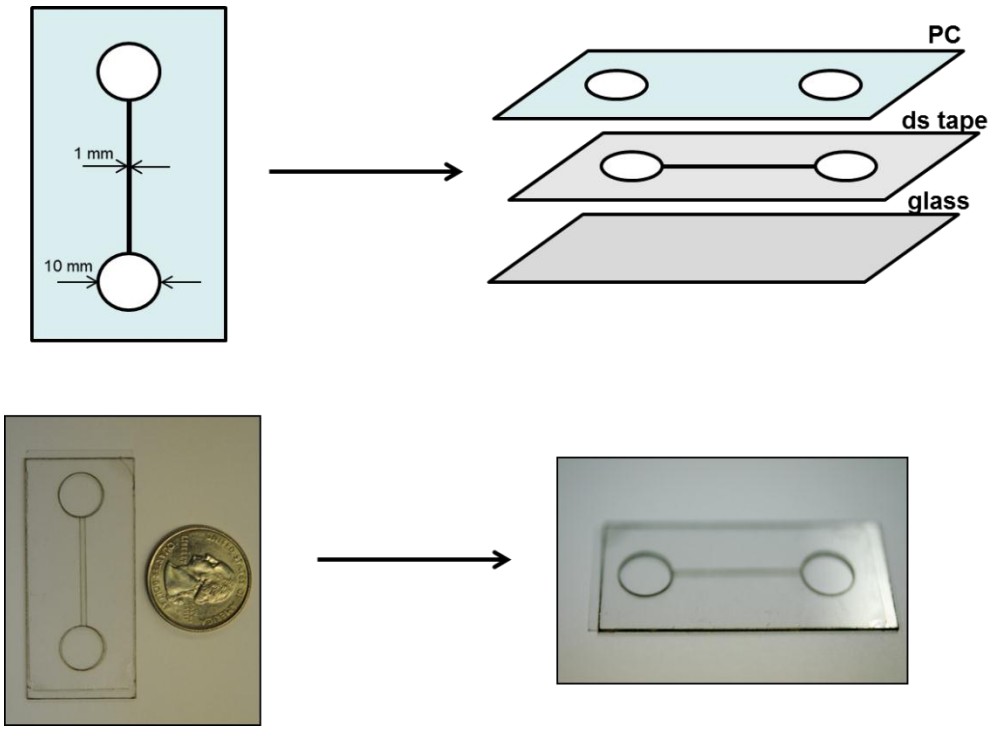

Figure 3.15. Microfluidic platform for trapping: top – conceptual design, bottom – actual platform.

The long-term goal for this part of the project is to combine microfluidic platform (to produce sensor particles on demand), trapping chamber and additional channels for cell introduction (Figure 3.17). Sensor particles will be trapped in one of the channels and injected into cells using another trapping laser to perforate the cell membrane and measure ion activities inside the cell.

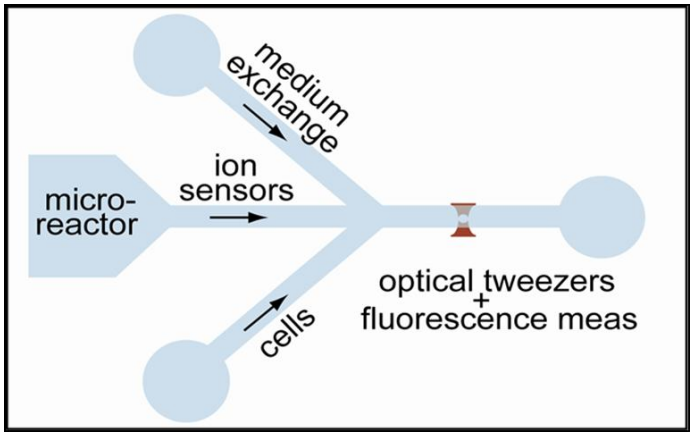

Figure 3.16. Explanation of the final device for intracellular ion activity measurements.

3.4. Conclusion

This work sought to address two main challenges in the process of synthesis ion-selective optodes: (1) fine control over the mixing process to allow for effective particle-size control, and (2) enhancing "effective" sensor lifetime by pushing production to the point-of-use, eliminating the need for long shelf-life. In the work presented here, we demonstrated that these two problems can be overcome by the use of a microfluidic approach to synthesis.

A microfluidic platform was successfully constructed using inexpensive polymer materials: cyclic olefin copolymer as the substrate for micromilled channels and polycarbonate/ polyether terephthalate for the clamping fixture. A syringe-pump with digital control provided for flow rate controlled reagent delivery.

It was shown that by varying polymer concentration in one of the mixing solutions, control over particle size could be achieved. It was also shown that the flow rates of the reactant solutions have no effect on the final size distribution, as the mixing process was dependent on diffusion rather than turbulent mixing in the flow rate range we studied.

3.5. References

[1] Bychkova, V., and A. Shvarev. "Fabrication of micrometer and submicrometer-sized ion-selective optodes via a solvent displacement process." *Anal. Chem* 81 (2009): 2325-2331.

[2] Karnik, Rohit, F. Gu, P. Basto, C. Cannizzaro, L. Dean, W. Kyei-Manu, R. Langer, and O. Farokhzad. "Microfluidic platform for controlled synthesis of polymeric nanoparticles." *Nanolett.* 8.9 (2008): 2906-2912.

[3] Buck, S., Xu H., Brasuel M., Philbert M., Kopelman R. "Nanoscale probes encapsulated by biologically localized embedding (PEBBLEs) for ion sensing and imaging in live cells." *Talanta* 63 (2004): 41-59.

[4] Lamonte, Ronald, and D. McNally. "Uses and Processing of Cyclic Olefin Copolymers." *Plastic Eng.* 56.6 (2000): 51-52.

CHAPTER 4

SUMMARY AND CONCLUSIONS

The main objective of this work was an introduction of improvements to the ion-selective optical sensors (ISO) applications. Two projects that were described above have common background – ISO – that our research group worked in for an extensive period of time. Together with their small size, ISO have one more advantage: they can be made selective to any ion that may be specifically complexed by an organic molecule of a certain design (ionophore). This research was devoted to cation-selective ISO and sodium selective optodes were taken as an example, since Na^+ is one of the essential ions in living organisms with defined concentration any changes in which serve as an indirect characteristic of illness.

First improvement that was made lies in the response mechanism of ISO. Organic dye (chromoionophore I) that is responsible for the detection of fluorescence signal from the optodes has an ability to photobleach in a short period of time upon excitation. To overcome this shortcoming we decided to incorporate quantum dots into the polymeric matrix.

QDs are known for their high resistivity to photobleaching and narrow emission spectra coupled with broad absorbance range in UV-region to enable excitation of a couple of different QDs with the same light. Thus, two types of QDs (to perform ratiometric measurements) were used for the project purposes – with emission at 545 and 605 nm – and they were both excited at 350 nm. Upon different experiments we discovered that QDs have a certain "safe" working range of pH and aggregate/precipitate at extremely acidic and basic conditions. Hence, the best option for QDs in to utilize them in applications where pH is close to neutral.

According to our idea, QDs should be excited at 350 nm, where chromoionophore I has no absorbance. The quantum dots were selected in a way that their emission peaks match the absorbance band of the fluorophore, permitting a two-step excitation of the fluorophore also known as the inner-filter effect. In this case the dye was indirectly excited with much softer [than from xenon microscope lamp] light emitted by QDs and photobleaching is successfully avoided (it is now possible to get a couple of spectra from the same optode particle).

Optodes were calibrated with respect to pH and sodium activity providing the same dynamic working range as optodes without QDs:

- at 1 mM Na^+ constant presence dynamic range of optodes response is pH 7.1 to 9.5;
- when keeping pH=7.5 sodium optodes show lower detection limit equal to $5x10^{-4}$ M and a dynamic range of $(5x10^{-4}) – (5x10^{-1})$ M.

Both calibration curves are in a good agreement with the theoretical prediction.

Second improvement deals with the method of optodes synthesis. Very simple one-step solvent displacement method of ISO fabrication was broadly studied by our group. This method is fast and reliable, but it is rather a challenge to control a particle dimensions in a bulk synthesis. Moreover, optodes have a short life-time due to the light caused degradation of incorporated organic dye and it is much better to synthesize them on demand. Thus was born the idea to introduce microfluidic platform to the synthesis of the particles.

The main challenge in this project was to find relatively chip and easy to process polymer that is resistant to THF (solvent that is used for the batch synthesis) or at least acetone (solvent that was tried for the batch synthesis once and promised to give the same results as THF). The vast majority of the polymers commonly used for microfluidic fabrication swell upon contact with organic solvents. After profound search we discovered a relatively new polymer – cyclic olefin copolymer (COC) – that is resistant to acetone (though, turns white after the exposure to THF) and utilized it for the fabrication procedure.

500 μm wide microfluidic channels of a special designed were micromilled on two plates of COC that later were physically bonded together with the help of custom-made fixture (transparent PC and opaque PET held together with the number of screws). Solutions were delivered by the syringe pump via PTFE tubing.

We learned that even though flow rate ratio of two reactant solutions (organic/polymer one with all the sensing components and aqueous solution of surfactant) does not affect the diameter of the particle, optodes size can be tuned by varying the concentration of the polymer in a one of the solutions.

After a number of synthetic trials it was found out that microfluidic platform serves as a reliable tool for the optodes fabrication on demand. Moreover, this platform can be coupled with another “chip” of a simplest design for the particle trapping by optical tweezers.

Laser tweezers are used to localize one particle and calibrate in right after the synthesis. Later, the same procedure will be used for the particle penetration inside a cell.

BIBLIOGRAPHY

[1] Langmaier J., E. Lindner "Detrimental changes in the composition of hydrogen ion-selective electrode and optode membranes." *Anal. Chim. Acta* 543 (2005): 156–166.

[2] Shvarev A., "Photoresponsive ion-selective optical sensor." *J. Am. Chem. Soc.* 128 (2006): 7138-7139.

[3] Michalet, X., Pinaud F., Bentolila L., Tsay J. , Doose S., Li J., Sundaresan G., Wu A., Gambhir S.,Weiss, S. "Quantum dots for live cells, in vivo imaging, and diagnostics" *Science* 307 (2005): 538-544.

[4] Ashkin A., "History of optical trapping and manipulation of small-neutral particle, atoms, and molecules." *IEEE J. Sel. Top. Quantum Electron.* 6 (2000): 841-856.

[5] Zhao, C., L. He, S. Qiao, and A. Middelberg. "Nanoparticle Synthesis in Microreactors." *Chemical Engineering Science* 66.7 (2011): 1463-479.

[6] Chien, R. "Hot Embossing of Microfluidic Platform." *Int. Comm. in Heat and Mass Transfer* 33.5 (2006): 645-53.

[7] Copperwhite, R., M. O'Sullivan, C. Boothman, A. Gorin, C. McDonagh, M. Oubaha."Development and Characterization of Integrated Microfluidics on Waveguide-based Photonic Platforms Fabricated from Hybrid Materials." *Microfluidics and Nanofluidics* 11.3 (2011): 283-96.

[8] Tesar, V. *Pressure-driven microfluidics* . Boston: Artech House, 2007.

[9] Tabeling, P.. *Introduction to microfluidics* . Oxford, U.K.: Oxford University Press, 2005.

[10] Brister, P. and K. Weston "Patterned Solvent Delivery and Etching for the Fabrication of Plastic Microfluidic Devices." *Anal. Chem.* **77** (2005): 7478-7482.

[11] Abgrall P., Low L., and Nguyen N. "Fabrication of planar nanofluidic channels in a thermoplastic by hot-embossing and thermal bonding." *Lab Chip* 7 (2007): 520-522.

[12] Lee, S., and N. Sundararajan. *Microfabrication for microfluidics* . Boston: Artech House, 2010.

[13] Chakraborty, S. *Microfluidics and microfabrication* . New York: Springer, 2010.

[14] Bruus, H. *Theoretical microfluidics*. Oxford: Oxford Univ. Press, 2008.

[15] Michler, P. *Single quantum dots: fundamentals, applications, and new concepts*. Berlin: Springer-Verlag, 2003.

[16] Masumoto, Y., and T. Takagahara. *Semiconductor quantum dots: physics, spectroscopy, and applications*. Berlin: Springer, 2002.

[17] Borovitskaya, E., and M. Shur. *Quantum dots*. River Edge, N.J.: World Scientific, 2002.

[18] Akmal, N., and A. Usmani. *Polymers in Sensors: Theory and Practice*. Washington, DC: American Chemical Society, 1998.

[19] Buck S., Koo Y., Park E., Xu H., Philbert M., Brasuel M., Kopelman R., "Optochemical nanosensor PEBBLEs: photonic explorers for bioanalysis with biologically localized embedding." *Curr. Opin. Chem. Biol.* 8 (2004): 540-546.

[20] Hisamoto, H. "Ion-sensitive and Selective Active Waveguide Optodes." *Analytica Chimica Acta* 342.1 (1997): 31-39.

[21] Alcock, S. and A. Turner. *In Vivo Chemical Sensors: Recent Developments*. Bedford, UK: Cranfield, 1993.

[22] Harris, D. *Quantitative Chemical Analysis*. New York: W.H. Freeman, 2003.

[23] Diamond, D. *Principles of Chemical and Biological Sensors*. New York: Wiley, 1998.